

Mathematical models for chemotaxis¹ and their applications in self-organisation phenomena

Kevin J. Painter^{a,b}

^a*Department of Mathematics & Maxwell Institute for Mathematical Sciences, Heriot-Watt University, Edinburgh, UK,
K.Painter@hw.ac.uk*

^b*Dipartimento di Scienze Matematiche, Politecnico di Torino, Torino, Italy*

Abstract

Chemotaxis is a fundamental guidance mechanism of cells and organisms, responsible for attracting microbes to food, embryonic cells into developing tissues, immune cells to infection sites, animals towards potential mates, and mathematicians into biology. The Patlak-Keller-Segel (PKS) system forms part of the bedrock of mathematical biology, a go-to-choice for modellers and analysts alike. For the former it is simple yet recapitulates numerous phenomena; the latter are attracted to these rich dynamics. Here I review the adoption of PKS systems when explaining self-organisation processes. I consider their foundation, returning to the initial efforts of Patlak and Keller and Segel, and briefly describe their patterning properties. Applications of PKS systems are considered in their diverse areas, including microbiology, development, immunology, cancer, ecology and crime. In each case a historical perspective is provided on the evidence for chemotactic behaviour, followed by a review of modelling efforts; a compendium of the models is included as an Appendix. Finally, a half-serious/half-tongue-in-cheek model is developed to explain how cliques form in academia. Assumptions in which scholars alter their research line according to available problems leads to clustering of academics and the formation of “hot” research topics.

Keywords: Pattern Formation; Patlak-Keller-Segel; Bacteria; Slime Molds; Development; Pathology; Ecology; Social Sciences; Social Clique Formation;

1. Introduction

The ability to detect and migrate in response to guidance cues is widespread and multifaceted, transcending scientific boundaries: similar mechanisms that orient immune cells towards infections help animals navigate towards feeding grounds; the friendly mechanisms essential for healing our tissues acquire a sinister face when corrupted in cancer development. Of the many cues available, movements induced by chemical factors (e.g. chemotaxis, chemokinesis) have received overwhelming attention, clear reflection of their ubiquitous nature (Figure 1a). As our ability to probe the molecular world has increased, phenomena such as chemotaxis have emerged as model processes to understand how cells and organisms read, respond and shape the sensory information in their environment.

A not insignificant contribution has arisen from mathematical and computational modelling. Early studies utilised continuous/population-level approaches, via partial differential equation (PDE) systems for the evolving densities of cells/organisms and the concentrations of attractants/repellents. Cheaper computational power has allowed the field to proliferate and diversify into increasingly sophisticated, specialised forms: for example, detailed molecular-level models to describe the complex signalling pathways or agent-based models that represent each individual. Consequently, models can be instilled with highly specific properties, fostering truly interdisciplinary studies that blend experiment and theory.

¹See Section 2!

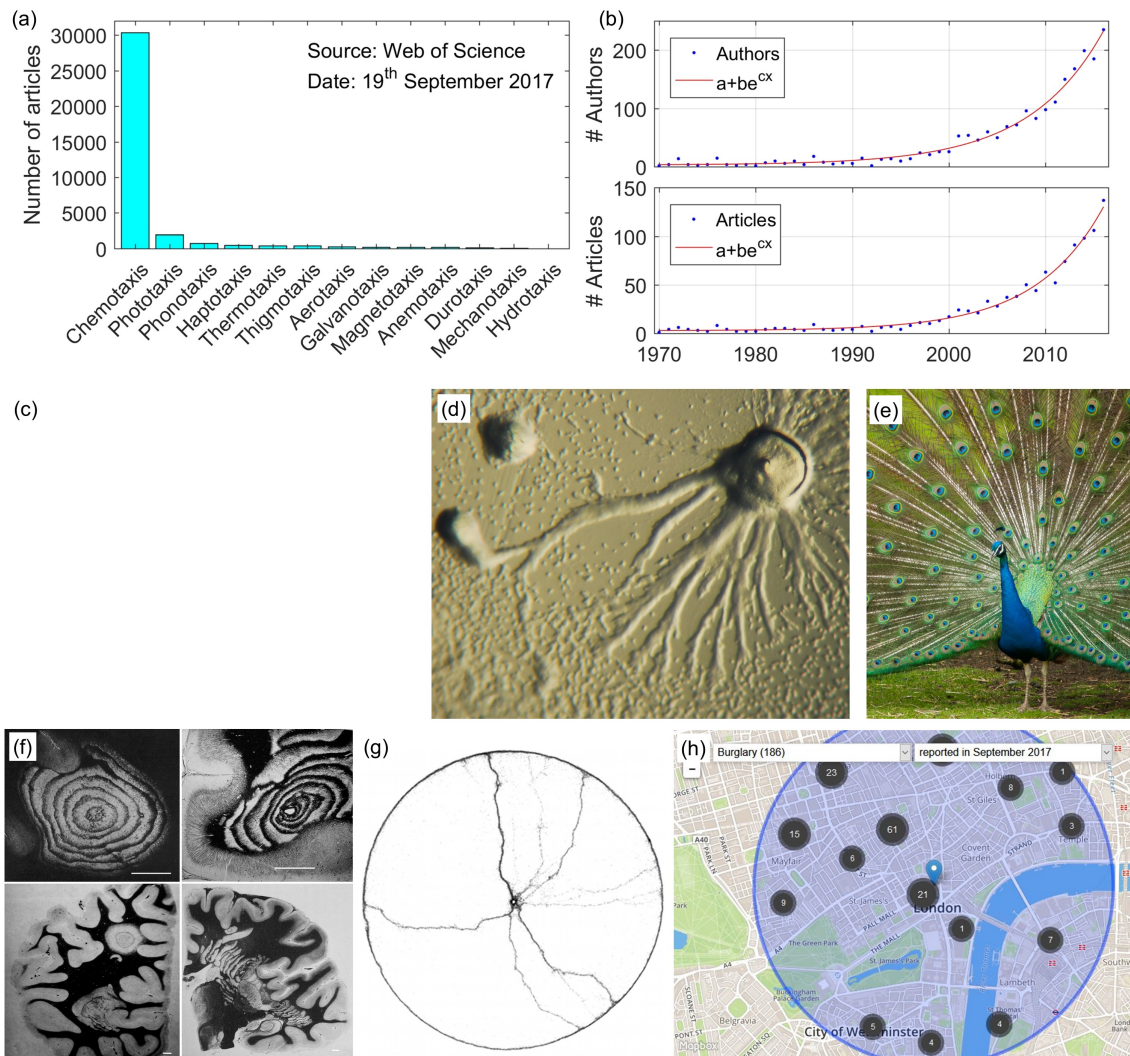


Figure 1: (a) Many “-taxis” cues exist, although chemotaxis is by far the most intensely studied. The bar chart reflects the number of articles (Web of Science Topic Search, 1900-September 2017) for aerotaxis (movement in the direction of oxygen gradients) anemotaxis (wind currents), chemotaxis (chemicals), galvanotaxis (electric fields), haptotaxis (adhesion gradients), hydrotaxis (moisture), magnetotaxis (magnetic fields), mechanotaxis (mechanical cues), phonotaxis (sound), phototaxis (light), rheotaxis (water currents), thermotaxis (heat), thigmotaxis (physical contacts). (b) An analysis of the number of articles (top) and the number of authors (bottom) citing Keller and Segel (1970) since 1970. Exponential fits provide an excellent match. (c-h) Examples of diverse areas in which PKS models have been applied: (c) Expanding rings of spots in *S. typhimurium*, (This figure has been removed due to permission rights); (d) *Dd* slime mold aggregation (Figure released into public domain, https://commons.wikimedia.org/wiki/File:Dictyostelium_Aggregation.JPG); (e) Feather placement during development; (f) Sclerosis patterns in neuropathologies (reproduced from Figure 1 of Khonsari and Calvez (2007), under the terms of a Creative Commons attribution license); (g) Trail formation in Argentine Ants (reproduced from Figure 1 of Perna et al. (2012), under the terms of a Creative Commons attribution license); (h) Crime hot spot formation (map generated from “Crime Map” facility available at <https://www.police.uk/>).

Yet, despite the trend towards fine detail, the ongoing development and exploration of continuous-level models remains a helpful, higher-level, approach. Benefiting from their roots in classic mathematics, they come with analytical tools capable of generating insight without recourse to heavy number crunching. For chemotaxis models, the system of PDEs formulated in Keller and Segel (1970, 1971a,b) and anticipated in Patlak (1953a,b) has proven particularly appealing. Composed of coupled reaction-diffusion-advection equations, it describes the evolving densities of one or more chemotactic population and its attractants/repellents, with a natural and logical description for the macroscopic *consequence* of chemotaxis. Defining $u(\mathbf{x}, t)$ to be the density of the chemotactic population at position $\mathbf{x} \in \mathbb{R}^n$ and time t and $v(\mathbf{x}, t)$ as its corresponding chemoattractant, the basic Patlak-Keller-Segel (PKS)² model is of the form

$$\begin{aligned} u_t &= \nabla \cdot (D_u(u, v)\nabla u - u\chi(u, v)\nabla v) + f(u, v), \\ v_t &= D_v\nabla^2 v + g(u, v). \end{aligned} \tag{1}$$

$f(u, v)$ and $g(u, v)$ respectively describe population and chemoattractant reaction kinetics, D_v is the chemoattractant diffusion coefficient and $D_u(u, v)$ and $\chi(u, v)$ respectively define population diffusion and chemotactic sensitivity coefficients. The key component is the advective *taxis-flux* choice $u\chi(u, v)\nabla v$: intuitively, this describes population drift up (or down) the direction of the local (chemical) gradient.

These models have readily been developed and applied to problems in fields ranging from ecology to economics, or cancer to crime, Figure 1c-h. In turn this has attracted analysts, imbuing the field with a sophisticated (though by no means complete) mathematical underpinning. Year on year numbers of publications/researchers citing one of the key early chemotaxis papers are closely fitted by exponential curves, Figure 1b, indicating this line of research continues to grow. Yet, modelling demands introspection: Vincent van Gogh said “Do not quench your inspiration and imagination; do not become the slave of your model”. We should not simply stick rigidly to a familiar form, blind to its limitations.

In this review, I evaluate the use of PKS models in describing chemotaxis (and other taxes), particularly focussing on examples of pattern formation/self-organisation³. I do not review the numerous excellent studies that primarily concentrate on their mathematical analysis: a number of reviews already cover these aspects in depth (Horstmann, 2003; Perthame, 2006; Hillen and Painter, 2009; Wang, 2013; Bellomo et al., 2015). Next, the fundamental modelling that led to (1) is reviewed and an overview given regarding its patterning behaviour. I then proceed field-by-field, beginning with its motivations in microbiology and sweeping across areas including developmental biology, immunology, cancer, ecology and the social sciences. For each case, the historical justification for chemotaxis is described and models are discussed; a compendium that contains many of these models is provided in the Appendix. Finally, I demonstrate how PKS models can continue to penetrate new areas, via a novel application to explain clique formation in research.

2. Navigating the nomenclature

Adopting uniform terminology in reviews of chemotaxis is a challenge: a varied nomenclature arises in a vast literature spanning microbiology, medicine and mathematics, embryology and ecology. Oxford English Dictionary’s rather precise definition “The orientated or directional movement of a motile cell or organism in response to a gradient of concentration of a particular substance; an instance of this.”, is countered by the vaguer “The movement of a microorganism or cell in response to a chemical stimulus” of Collins⁴. Yet, stating one correct definition ignores the historical perspective and vagaries of distinct fields.

²These are often simply stated as the Keller-Segel equations in the literature. Here I use PKS to reinforce the connection between the distinct approaches employed by Patlak and Keller-Segel during early modelling.

³I apologise to the many authors whose relevant work has not been cited for conciseness. In mitigation, a search on “chemotaxis” in Web of Science generates more than 30,000 studies dating back to 1900...

⁴“Chemotaxis”, <https://www.oed.com> and <https://www.collinsdictionary.com>.

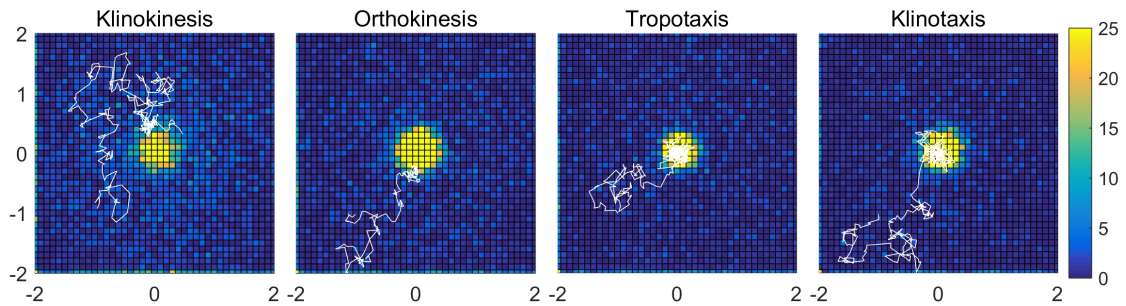


Figure 2: Results of agent-based simulations, where individuals respond to a chemical cue peaking at the origin (e.g. chemical injected from a micropipette). Agents move via a stochastic velocity-jump random walk (Othmer et al., 1988), where particles perform: (i) klinokinesis, in which turning frequency increases with concentration; (ii) orthokinesis, in which speed decreases with concentration; (iii) tropotaxis, in which orientation is biased according to an instantaneous chemical gradient; (iv) klinotaxis, in which orientation is biased according to a gradient calculated from separate locations at successive time points. For each case the path of a single agent (white track) and the histogram (heat map indicates particle number/box) for the particle distribution is plotted, the latter following evolution to a “steady state” distribution (10,000 individuals).

Chemotaxis was first described for bacteria and other single cells more than a century ago, following pioneering studies of Engelmann (1881a,b, 1883) and Pfeffer (1884). Attributing this to bacteria *steering towards* the chemical signal – an implied *directed* migration – the latter coined the term chemotaxis. This steering hypothesis was later abandoned by Pfeffer, but *-taxis* had entered common parlance. In the following years a variety of suffixes (*-taxes*, *-kineses* and *-tropisms*) were attached to movement and/or growth processes, but, as studies surged and distinctions noted, a more formal classification was demanded. Kühn’s (Kühn, 1919) early systematic classification was superseded by that of Fraenkel and Gunn (1940), and the latter has (by and large) stuck for animals and certain cells, such as leukocytes (see Keller et al., 1977).

A *-kinesis* is an *undirected* movement response, i.e. there is no orientation according to the stimulus. *Kineses* can be subclassified into *orthokinesis* if the intensity of the signal triggers a change in the speed (or frequency) of locomotion, or *klinokinesis* if the intensity alters the rate of turning. A *-taxis* forms a *directed* movement response, such that the cell/organism orients with respect to the signal. The response is positive or negative if the orientation is towards or away from the source. *Taxes* subclassify into *tropotaxis* if the individual orients by directly measuring a spatial gradient, or *klinotaxis* if a gradient is indirectly measured, for example by comparing signal intensities at two different locations and at successive time points. Different mechanisms place different demands on sensory skills: tropotaxis would require (at least) two, spatially separated, receptors (e.g. two antennae) while klinotaxis requires just one, but with an additional “memory”. Regarding the original usage of “chemotaxis”, the bacteria of Pfeffer turned out to use a form of klinokinesis rather than taxis. Nevertheless, chemotaxis remains the common term in microbiology to describe their behaviour.

While the above classes all describe different *microscopic* behaviours, *macroscopic* outcomes can turn out to be similar: for example, all can induce a population to accumulate at the source of some chemoattractant if suitable rules are adopted, Figure 2. Chemotaxis is often more broadly used to describe an observed macroscopic movement flux with respect to a chemical gradient, as in the original observations of Pfeffer. Given the spectrum of studies covered, I will often adopt this looser macroscopic interpretation of chemotaxis, unless a more specific attribution has been shown.

3. Continuous models of chemotaxis

Historical reviews of continuous chemotaxis models must consider the landmark works of Patlak (1953a,b) and Keller and Segel (1970, 1971a,b). These studies have piqued interest in numerous fields, sparked volumes of analysis and form part of the infrastructure of spatial movement modelling. They also elegantly illustrate distinct modelling approaches.

3.1. Patlak

Patlak's modelling focussed on the individual perspective: given a stochastic random walk description for the path traced out by some particle, what is the PDE that governs the population-level distribution? Karl Pearson had coined the term random walk almost half a century earlier, posing his famous drunkard's walk⁵ problem (Pearson, 1905) when modelling mosquito population dynamics (Pearson, 1906), but Patlak strove to extend the theory to include non-independence between successive steps (so that individuals persisted in a given direction) and the impact from external biases. The latter could easily stem from chemotaxis, although the term is not even mentioned in Patlak (1953a): applications to organism movement, in particular klinokinesis, were considered in Patlak (1953b).

Avoiding details – an excellent, accessible description of Patlak's modelling is found in Turchin (1991) – Patlak derived a modified Fokker-Planck equation in the diffusion approximation to his random walk,

$$u_t = \nabla \cdot [F_1(\cdot)\nabla(F_2(\cdot)u) + F_3(\cdot, \varepsilon)u] .$$

F_1, F_2 and F_3 are functions explicitly defined in terms of the random walk: speeds, run durations and lengths, persistence factor and the external bias ε ; the latter offers the route for including taxis biases.

3.2. Keller and Segel

The initial modelling of Keller and Segel drew inspiration from macroscopic phenomena: the suggested driving role of chemotaxis in *Dictyostelium discoideum* (*Dd*) aggregation (Keller and Segel 1970, see Section 4) and *Escherichia coli* (*E. coli*) bacteria band formation (Keller and Segel 1971b, see Section 5). These are phenomena at a population scale, invoking maybe a million cells or more, and a classical approach centred on conservation of mass was adopted. In its macroscopic sense, (positive) chemotaxis generates a population drift up concentration gradients and accumulation at attractant sources. Hence, a logical chemotactic flux is in the direction of the gradient, i.e.

$$J_{\text{chemotaxis}} = u\chi(u, v)\nabla v .$$

The sensitivity function $\chi(u, v)$ can depend on both cell and attractant densities, or even their spatial and/or temporal derivatives. Assuming only the above for the flux would state that chemotaxis is perfect: movement exactly in the direction of the attractant gradient. More realistically, paths deviate due to extrinsic/intrinsic stochasticity and the above is appended with a Fickian diffusion flux. Subsequently adding population kinetics and equations for the chemoattractant then gives rise to the PKS model (1).

3.3. Explicit derivations of PKS models

The different modelling approaches echo the distinct definitions of chemotaxis: phenomenological/mass conservation methods do not address individual subtleties, rather they capture chemotaxis in its macroscopic spirit; a random-walk derived model can account for movement idiosyncrasy, for example the focus on klinokinesis in Patlak (1953b). Despite this, they share essential features: a diffusive term stemming from randomness/uncertainty and advection according to the direction of external bias. Yet the connection

⁵The name derives from an exchange in the journal *Nature* between Pearson and Lord Rayleigh, where the problem was first proposed.

to the PKS model is hinted rather than direct, and we mention further works that formally establish the link. Alt (1980) built on Patlak’s work, constructing a random walk model whereby runs alternate with reorientations and deriving a differential-integral equation for the density at position \mathbf{x} , time t , moving in direction θ and having started a run at time τ . A PKS equation was obtained for the macroscopic population density in certain limits. Othmer et al. (1988) formally laid out space-jump and velocity-jump processes as conceptual random walk models for biological motion: in the former, movement occurs through a sequence of positional jumps in space (instantaneous transfer between two separated points), the latter generalised the descriptions of Patlak and Alt. In the process an alternative “mesoscale” continuous model was clarified, the *transport equation* that stemmed from the velocity-jump process: an evolution equation for a population parametrised with respect to position, time and velocity. While more complex than the PKS model, this has been enthusiastically adopted in many studies, including chemotaxis modelling (e.g. see Rivero et al. 1989; Othmer and Hillen 2002; Dolak and Schmeiser 2005; Saragosti et al. 2011; Pineda et al. 2015), blending advantages of a continuous framework and closer connection to the microscopic setting.

For space-jump processes, Stevens and Othmer (1997) explored the continuous equations derived for subtly varying chemosensitive movement rules: models were of general PKS form, but with differing diffusion/taxis terms that could translate into profoundly distinct behaviour. The connection from velocity-jump processes to PKS models initiated in Patlak (1953a) and Alt (1980) continued – see the review by Othmer and Xue (2013) – to generate insight into when and if PKS models can provide a reasonable approximation. In bacteria with well understood signalling and motion closely approximated by a velocity-jump process, such as *E. coli*, one can even link parameters and functions characterising molecular signalling and motor control to the parameters and functions that define diffusive/chemotactic sensitivity terms in a PKS model (Othmer and Xue, 2013). Moreover, novel and interesting variations can emerge, such as the “perpendicular gradient following” that arises from swimming biases (Xue and Othmer, 2009), fractional operator terms due to non-Poisson type turning rate distributions (Estrada-Rodriguez et al., 2017) or “flux-limited” forms (Perthame et al., 2018). Noteworthy, the above derivations rely on ignoring interactions and Stevens (2000) is noted for providing the first rigorous derivation of a PKS equation for a population of stochastic (weakly) interacting particles. Further derivations of PKS models from stochastic models include those of Newman and Grima (2004); Alber et al. (2007); Chavanis (2010). Reductions to a simple PKS model have also been made from more detailed continuous models, such as incorporating receptor binding and transport (Sherratt, 1994) or through multiphase modelling techniques (Byrne and Owen, 2004).

3.4. Self-organisation and patterning

The model (1) is elegant and intricate: superficially simple, yet capable of complex dynamical behaviour. Undoubtedly, its self-organising capacity has sparked the most interest and, indeed, was the primary question of Keller and Segel (1970). The most carefully studied PKS model contains autotactic feedback, whereby a population produces its own attractant. A “minimal” model comprises of constant/linear functional forms in (1): D_u, χ constants, $f(u, v) = 0$ and $g(u, v) = \alpha u - \beta v$, where α and β respectively describe the rates of attractant production by the population and decay. Linear stability analysis applied about the uniform/homogeneous solution generates the *necessary* instability condition

$$\chi \alpha u_s > \beta D_u,$$

where u_s is the density of the population at uniform equilibrium. In essence, if a sufficiently dense population (u_s) shows sufficiently strong chemotaxis (χ) and produces sufficient attractant (α) then the stabilising effects of random motion (D_u) and chemoattractant decay (β) are overcome. Further conditions are derived for specific domains and boundary conditions.

The above intuitively generates symmetry breaking, so what curbs the process? Do smooth, stationary density distributions form, do they continuously evolve in time or does the population collapse in on itself *ad infinitum* (“blow-up”)? The answers are non-trivial and explain why PKS models have generated so much analytical interest. Other reviews explore this subject in depth (most recently Bellomo et al. 2015,

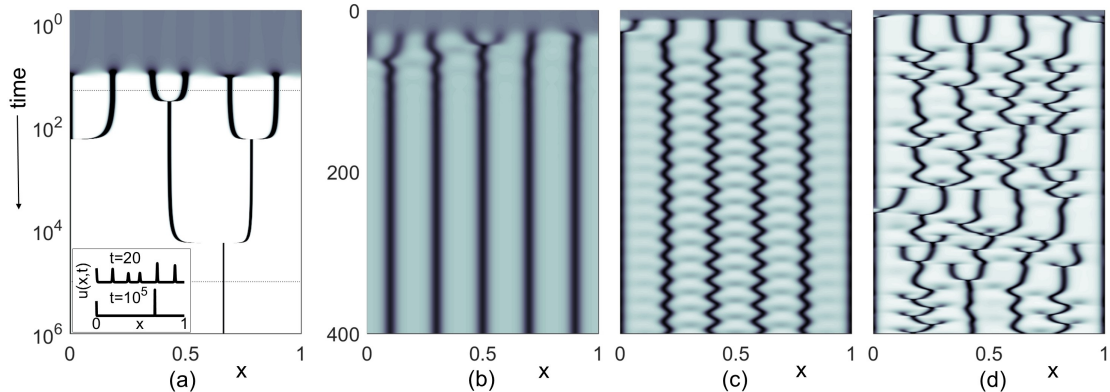


Figure 3: Examples of spatio-temporal patterns in simple 1D chemotaxis models. Grayscale indicates population density from $u = 0$ (light gray) to $u \geq 2$ (black). Here $D_u = D_v = 0.001$ and $g(u, v) = u - v$. (a) Merging dynamics, for $f(u, v) = 0$ and $\chi = 0.005$. (b-d) Stationary, oscillating and chaotic patterns for $f(u, v) = u(1 - u)$ and (b) $\chi = 0.005$, (c) $\chi = 0.006$ and (d) $\chi = 0.008$. The inset of (a) shows the cell density profile at $t = 20$ (incipient stage of pattern formation) and $t = 10^5$ (following multiple merging events). Simulations solved on a 1D domain $[0, 1]$ with zero-flux boundary conditions.

but see also Horstmann 2003; Perthame 2006; Hillen and Painter 2009), so here we confine to a superficial account. The question of global existence *vs* blow-up has been extensively studied: in the minimal model solutions exist globally in 1D, but for 2D (and above) blow-up occurs if the population exceeds a critical density. Blow-up indicates the aggregating tendency, yet is problematic: first, populations do not form singularities as, even under dense aggregation, an individual’s finite size (for one) precludes total collapse; second, from a numerical/modelling perspective it limits the ability to study dynamics post-aggregation. Blow-up can be prevented through *appropriate* regularisation (Hillen and Painter, 2009), by which we mean density bounds should arise from natural limiting features: for example, *E. coli* aggregates can occur at loosely-packed levels (Mittal et al., 2003), suggesting that the mechanisms that limit cell densities are not (solely) the result of volume exclusion.

If patterning occurs, what form? Again the answers are not straightforward. As opposed to the large literature on blow-up/global existence, relatively little is known on the form and stability of solutions to chemotaxis models. For a 1D domain, solutions to the minimal model are “spiky” (Lin et al., 1988), with numerical simulations on largish domains generating multiple (quasi) regularly-spaced aggregate spikes, each supported by localised attractant production. Yet attractant produced by one aggregate diffuses to neighbours, they mutually attract and merge until a single “winner” remains, see Figure 3a. Similar behaviour occurs in related models, such as the “volume-filling” model, where Potapov and Hillen (2005) have numerically explored metastability properties. Essentially, coarsening results from transient passage along metastable multi-aggregate steady states until resting on a stable boundary aggregate; Dolak and Schmeiser (2005), using singular perturbation methods, showed that neighbouring peaks must be sufficiently close to sense each other and merge. Similar properties for the minimal model have been explored in Hillen and Potapov (2004) and Kang et al. (2007). In the latter asymptotic methods were used to construct a central spike solution, shown to possess metastability and drift exponentially slowly to the boundary. For further results on the form and stability of patterned solutions to PKS models, see for example Wang (2013); Chen et al. (2014); Zhang et al. (2017). The introduction to Wang (2013) is highlighted for containing a review of earlier results.

Obtaining stable multiple aggregate solutions, therefore, seems to demand further factors. Adding population kinetics is one method, with classic choices including logistic or cubic forms (Mimura and Tsujikawa, 1996). The former choice has received particular attention and does indeed appear to stabilise

multi-aggregate solutions, but only for certain parameter sets. Others can lead to highly dynamic time-periodic or chaotic solutions, where merging alternates with newly forming aggregates (Aida et al., 2006; Wang and Hillen, 2007; Painter and Hillen, 2011; Banerjee et al., 2012; Ei et al., 2014), see Figure 3b-d. As illustrated later, other models have been shown to generate a variety of further, sometimes bizarre, pattern forms. Stable multi-aggregate solutions also appear possible through dual attractant-repellent systems, where a combination of short-range attractant and long-range repulsion appears to stabilise multi-aggregate solutions (Luca et al., 2003). In short, chemotaxis models are capable of wide-ranging dynamical behaviour.

4. Applications in *Dictyostelium* self-organisation

4.1. Background

Cellular slime molds, the “social amoebae”, form a celebrated group of soil-dwelling microorganisms whose rise to prominence stems from a life cycle that straddles individuality and multicellularity. The model organism *Dd*⁶, in particular, serves as a textbook example of self-organisation, see Bonner (2009). In its vegetative phase individual cells swarm, consume and divide until food is depleted. Starvation heralds a remarkable shift, as the dispersed population accumulates into a multicellular entity that passes through various stages: differentiating and sorting into pre-spore and pre-stalk types, transforming into a migrating “slug” and eventually a fruiting body. This final act invokes apparent altruism, with spore cells shaped into a ball, encased and suspended by a thin trunk of sacrificed stalk cells⁷. Transport of spores to a new location restarts vegetative growth.

Cells collect over an “aggregation territory”, maybe up to a centimetre or so across, with inward movement not smooth but in a sequence of pulses that initiate centrally and radiate outwards (Arndt, 1937). Closing on the aggregate, cells condense into streams that form a branched network, see Figure 1d. A role for chemotaxis was proposed in the 1940s (Runyon, 1942) and gained substance with the trailblazing work of Bonner⁸ (Bonner and Savage, 1947): specifically, a diffusing attractant, generically termed acrasin, was suggested to guide cells into a developing mound. Shaffer (1953, 1956) verified that mounds produced both acrasin and an “acrasinase” that degraded it, leading to a proposed relay system (Shaffer, 1957; Gerisch, 1968; Cohen and Robertson, 1971a,b): (i) central pacemaker cells periodically release an acrasin pulse; (ii) nearby cells respond by both moving in its direction and releasing further pulses; (iii) the next cell is stimulated and so forth. Acrasinase wipes the slate clean, clearing excess extracellular acrasin in advance of the next wave. In essence, *Dd* forms an excitable medium (Durstun, 1973). Molecular identities – acrasin was found to be 3'-5'-cyclic adenosine monophosphate (cAMP) (Konijn et al., 1968) and acrasinase a type of phosphodiesterase (Chang, 1968) – and increasingly sophisticated observations verified the relay theory (Alcantara and Monk, 1974; Shaffer, 1975; Gross et al., 1976): for one of the first times, cell signalling was dissected into its raw ingredients and mechanisms. Subsequent decades have generated an increasingly nuanced understanding of *Dd* chemotaxis, see the recent reviews Nichols et al. (2015); Bretschneider et al. (2016).

As eukaryotes, *Dd* cells move similarly to many human cells: frequent membrane extensions (pseudopods) form that transiently anchor to the substrate/other cells and generate traction for motion. In the absence of cAMP, pseudopods extend in random directions, but localised detection leads to localised extension. Cells can directly detect a spatial chemoattractant gradient, possibly as low as 2% front to back, and internal signalling amplifies the initial gradient to create a clear directional polarity (Van Haastert and Devreotes, 2004). Besides the aggregation of dispersed cells, chemotaxis also directs other aspects of the life-cycle: pre-aggregation, swarming vegetative cells exhibit chemotaxis to folates (secreted by certain bacteria prey)

⁶ First identified in the 1930s by Raper (1935) when searching through camel dung, see Durstun (2013).

⁷ In fact, *Dd* are not so magnanimous: “cheating” is rife and certain clones will contribute less than their share to the stalk (Strassmann et al., 2000).

⁸ Bonner’s videos (available on Youtube) were highly popular, with famous visitors to the lab including Albert Einstein.

(Pan et al., 1975); post-aggregation cAMP chemotaxis plays a critical role in mound and slug dynamics, with differential chemotaxis sorting pre-spore and pre-stalk cells (Matsukuma and Durston, 1979; Sternfeld and David, 1981; Traynor et al., 1992) and cAMP waves continue to propagate through the mound and slug (Dormann and Weijer, 2001).

4.2. Modelling

The above process generated source inspiration in the early chemotaxis modelling of Keller and Segel (1970). At the time, chemotaxis/acrasin interactions were known to be necessary, but were they sufficient? Specialised “founder cells” were speculated to act as mound initiators (e.g. Shaffer 1961), but were they essential? Could aggregation occur without cell heterogeneity? Modelling allows hypotheses to be stripped to their bare essentials to address such questions. Keller and Segel’s model (see (A1) in the model compendium, Section Appendix A) consisted of 4 variables: amoebae, and concentrations of acrasin, acrasinase⁹ and the complex formed following their reaction. Pseudo-steady state approximations allowed further reduction to a familiar two variable model for amoebae and their attractant, (A2). A Turing-type (Turing, 1952) stability analysis¹⁰ was subsequently employed to show a dispersed population could self-organise, given: (i) sufficient sensitivity to the attractant; (ii) cells produce sufficient acrasin; (iii) acrasinase degrades acrasin sufficiently fast. Bonner’s lab indeed found that sensitivity to cAMP and its production rate (dramatically) increased at the inception of aggregation.

The model was simple even for its time: in their words, based on “simplest possible assumptions consistent with the known facts”. Thus, it did not account for a more sophisticated periodic cAMP relay system and was perhaps more appropriate for related species (such as *Dictyostelium minutum*) that secrete cAMP steadily and produce simpler, smoother aggregations. Its modesty, though, is the base of its appeal: it showed that an entirely homogeneous population could organise through simple self-secretion of an attractant, i.e. the founders could be the entire population. Nanjundiah (1973) performed a more detailed analysis, suggesting that it could potentially give rise to streaming/branching type phenomena. Following years witnessed significant modelling, but usually targeted at the signalling pathways necessary for the periodic cAMP relay waves: a comprehensive review can be found in Othmer and Schaap (1998). Höfer *et al* (Höfer et al., 1994; Hofer et al., 1995; Höfer et al., 1995) merged more refined signalling with a PKS model for chemotactic cell movement (A3); spatial cAMP signalling had been studied, but for “immobilised” cells (Tyson et al., 1989; Monk and Othmer, 1990). Remarkably, the model replicated many complex *Dd* aggregation phenomena, from outwardly spiralling waves of cAMP to streaming and branching of cells as they approached the aggregate. Other continuous models have also been developed for *Dd* development, particularly to explain slug regulation and movement (Pate and Othmer, 1986; Odell and Bonner, 1986; Vasiev and Weijer, 2003; Pineda et al., 2015), although their underlying model framework is somewhat distinct from the PKS system.

Concurrently, various groups (e.g. Van Oss et al. 1996; Dallon and Othmer 1997; Savill and Hogeweg 1997; Palsson and Othmer 2000; Marée and Hogeweg 2001) were formulating “hybrid” models: agent-based models coupled to continuous equations for chemicals. The cell description varied, but models shared a common capacity to incorporate explicit microscopic detail and numerous features of *Dd* morphogenesis could be captured. The modelling shift towards the cellular/microscopic scale followed the greater biology focus at this level: population-scale modelling of *Dd* chemotaxis via continuous approaches has somewhat taken a backseat in recent years, although see Ferguson et al. (2016) for a recent example.

⁹Although formally identified at the time, this was recent and generic designations were retained in the model description.

¹⁰Turing’s classic theory was relatively new at the time.

5. Applications in Bacterial Chemotaxis

5.1. Background

The studies of Engelmann and Pfeffer (see Berg 1975 for a review) formed initial steps along the road to our most well understood signalling system: bacterial chemotaxis in *E. coli*. Swimming *E. coli* (and certain other bacteria) alternate between “runs” and “tumbles”, powered by the rotating flagella attached to their cell surfaces. During the former, anti-clockwise rotations bundle the flagella to generate almost straight-line swimming; tumbling is induced by clockwise rotation, with flagella flaying out so that the cell spins quasi-randomly. Their chemotactic properties were elegantly studied by Adler in the 1960s (Adler, 1966, 1969) who, by linking extracellular chemoattractants (repellents) to specific cell surface receptors (Adler, 1969), lay the groundwork for discerning how a cell perceives its chemical landscape. The chemoreceptor array stimulates intracellular signalling, mediated by a family of “Che” molecules, to modulate flagella rotation: see Wadhams and Armitage (2004); Parkinson et al. (2015) for reviews. *E. coli* are considered too small to discriminate an actual spatial gradient (but see Thar and K uhl 2003). Chemotaxis rather occurs via “klinokinesis with adaptation”: temporal calculations in which the absolute extracellular chemical concentration feeds into the tumbling frequency (Schnitzer et al., 1990). The interval between tumbles lengthens when concentration increases so that, overall, more time is spent moving up a gradient than down it and cells accumulate near the attractant source. Longer timescale adaptation resets the system, extending the concentration range for effective chemotaxis. Summarising, *E. coli* do not perform “true chemotaxis” under its formal microscopic definition.

Chemotactic studies have contributed to a perceptual shift of bacteria as highly sophisticated, capable of intercommunication (Shapiro, 1998). Self-organisation phenomena abound and multicellular patterns are formed of astonishing intricacy, see Ben-Jacob et al. (2000); Kaiser (2003). The experiments of Adler revealed chemotactic group behaviour in *E. coli*, whereby high density travelling bands (or spreading rings) formed following insertion of a population into nutrient containing capillary tubes (or petri-dishes) (Adler, 1966). Chemotactic-driven self-organisation was demonstrated by Budrene and Berg (1991, 1995), using *E. coli* and *S. typhimurium* populations. Under certain nutrient environments patterns formed in the wake of outward radiating waves, including stripes and spots of high bacterial density.

5.2. Modelling

Explaining the bacteria bands observed in Adler’s experiments had been another motivating factor for early modelling (Keller and Segel, 1971b), and various further studies have explored this phenomenon via PKS models (e.g. Lapidus and Schiller 1978; Lauffenburger et al. 1984; Brenner et al. 1998; Croze et al. 2011); we also refer to Wang (2013) for a review of the mathematics behind travelling waves in chemotaxis systems. The use of PKS models to describe the self-organisation phenomena observed in Budrene and Berg (1991, 1995) has been a fertile research area, see Woodward et al. (1995); Tsimring et al. (1995); Tyson et al. (1999a,b); Polezhaev et al. (2006); Aotani et al. (2010). In an early application, Woodward et al. (1995) integrated experiment and theory to determine whether *S. typhimurium* patterns could be attributed to chemotaxis: experiments reveal spots or solid rings as the nutrient (succinate) concentration varied (Figure 1c), while biochemical analyses revealed aspartate (a known chemoattractant) secretion by the aggregates. A bare-bones PKS model for bacteria and chemoattractant (B1) was able to recapitulate the experimental observations, capturing the pattern transition as the nutrient level changed; see Figure 4 for an illustration. Thus, chemotaxis may be a sufficient mechanism for this process of self-organisation. Further studies expanded to include additional factors, for example evolving nutrient dynamics (Tsimring et al., 1995; Tyson et al., 1999a,b; Polezhaev et al., 2006; Aotani et al., 2010), cell transitions into vegetative form (Tsimring et al., 1995; Polezhaev et al., 2006; Aotani et al., 2010) and the inclusion of waste products (Tsimring et al., 1995): see models (B2-B6). Consequently, many of the even more spectacular observations could be captured. An apparently chaotic pattern of *E. coli* merging/emerging events has been modelled via a PKS system in Baronas et al. (2015).

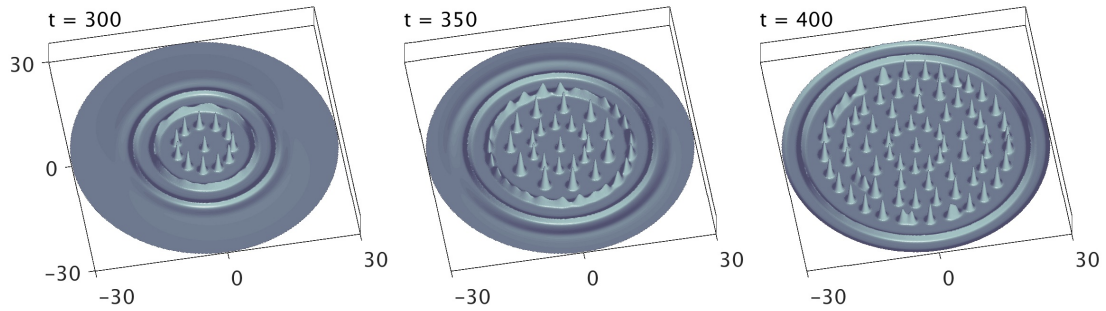


Figure 4: An expanding pattern of spotted rings in the model (B1), where we set $\chi = 3, k_1 = 2, k_2 = 0.03, k_3 = 1, s = 2, k_4 = 0.5, k_5 = 1, k_6 = p = 0, D_u = 0.1$ and $D_v = 0.3$. The food source is set at $s = 2$ and we solve on a circular domain of radius 30 with zero-flux boundary conditions at the edge. Solutions plot bacteria densities at $t = 300, 350, 400$, following the initial placement of a small compact population at the origin.

Bacillus subtilis swimming within fluid environments can create highly intriguing dynamics, such as falling plumes and aggregates at the contact lines of thin fluid layers separating a solid substrate and air (Hillesdon et al., 1995; Tuval et al., 2005). Bacteria swim upwards through a response to oxygen (aerotaxis), which they consume, before gravitational forces push them downwards. This overall motion results in bioconvection, a bacteria-driven fluid flow that convects both the bacteria and oxygen. A chemotaxis-flow model, whereby a PKS model is coupled to a fluid flow equation (model B8), was developed in Hillesdon et al. (1995) and has been readily applied (e.g. Tuval et al. 2005; Chertock et al. 2012; Lee and Kim 2015; Deleuze et al. 2016 amongst others) to describe flow-driven bacteria pattern formation.

Contemporaneous to much of the above, a large literature has emerged where the modelling is focussed at the molecular scale: see Tindall et al. (2008b,a); Othmer et al. (2013); Tu (2013) for reviews. As for *Dd*, discrete and/or hybrid approaches have become increasingly popular for obtaining population-level insights while retaining intracellular/cellular scale details: Bray et al. (2007); Xue et al. (2011) give two examples of this large literature. Yet, the potentially vast size of colonies still preclude their usage for entire populations, which can easily run to billions. Continuous models therefore remain a valuable tool, but quantitative comparison will increasingly demand their construction according to relevant microscopic details.

6. Applications in embryonic development

6.1. Background

The striking semblance of *Dd*'s lifecycle to development was noted in the seminal 1950s textbook by Waddington (1956), with speculation that similar mechanisms could act. Embryogenesis is, perhaps, the most remarkable direct example of self-organisation: a fertilised cell doggedly transforms itself into a multicellular organism, orchestrated by proliferation, migration, differentiation, apoptosis, intra/extracellular signalling and shaped by internal and external mechanical forces. It is an area rife with famous theories, from Turing's reaction-diffusion mechanism (Turing, 1952) to pre-pattern models based on position information (Wolpert, 1969).

Development is pragmatically studied piecemeal: the transformation of the early embryo into a multi-layered tissue structure during gastrulation; laying the developmental blueprint during segmentation/somitogenesis; within-tissue patterning of individual organs such as the central nervous system, skin, lungs and vasculature. *Definitive* demonstrations of chemotaxis are difficult (Shellard and Mayor, 2016):

cultivation and study *in vitro* is possible, but determining whether the same behaviour occurs *in vivo* is non-trivial. These difficulties aside, a hypothesised role for chemotaxis has a history stretching back more than a century. Ramòn y Cajal¹¹ proposed that chemotaxis¹² may be key to establishing interneuronal connectivity during nervous system development (Ramon y Cajal, 1892), a theory that lay dormant for decades before spectacular revival in the 1990s when various molecular families (e.g. netrins, semaphorins) were identified with attractive/repulsive guidance information: the review in Tessier-Lavigne and Goodman (1996) chronicles the lead-up to these fundamental discoveries, while a more recent perspective is provided in Kolodkin and Tessier-Lavigne (2011). In the 1940s, Twitty proposed that (negative) chemotaxis could control dispersal of pigment cells from the neural crest (Twitty, 1944; Twitty and Niu, 1948, 1954) and, while this remains unverified (Erickson and Olivier, 1983), other neural crest populations can be chemotactically guided by factors including VEGF (McLennan et al., 2010) and Sdf1 (Theveneau et al., 2010) (see also Shellard and Mayor 2016). Other promising cases of chemotaxis during development include border cell migration (Montell et al., 2012) and gastrulation (Yang et al., 2002).

The extent to which chemotaxis occurs in the periodic patterning processes beloved by mathematical biologists is difficult to deduce. Generation of repeating patterns is a common theme – examples include skin structures (pigmentation patterns, hairs, feathers, scales, sensory bristles), tooth morphogenesis, taste buds and limb skeletal structures — yet unravelling enough of the complex molecular/cellular/mechanical interactions and making firm statements is a challenge. A promising example lies in feather/hair arrangements. Feathers emerge from an orderly arrangement of skin placodes, each marked by epidermal signalling underlain by dermal cell aggregation. In chickens, FGFs (Song et al., 2004; Lin et al., 2009; Ho and Headon, In preparation) and BMPs (Michon et al., 2008) are potential chemotactic factors that may act to guide mesenchymal cells into the initial clusters; in mammals, FGF-dependent cell clustering occurs prior to hair follicle formation (Glover et al., 2017). Yet these remain examples of chemotaxis under its macroscopic guise: a clustering of cells according to a molecular distribution and the precise mechanisms involved are uncertain. Additional complications lie in the likely involvement of other pattern forming mechanisms, such as those based on activator-inhibitor principles (for a review, see Painter et al. 2012).

6.2. Modelling

The mechanochemical framework proposed by Murray, Oster and others in the 1980s (Murray, 2003) offered a general method for describing the interactions between motile cells and their environment: movement due to force-based interactions between cells and the surrounding extracellular matrix (ECM) and PKS-type fluxes to describe chemotactic, haptotactic *etc* responses were included. Numerous development-oriented applications have been made (e.g. see Murray 2003), including mesenchymal condensation and accumulation of chondrocytes during bone formation (chondrogenesis). Of course, most such models do not rely on chemotaxis alone: in fact spatial structure can potentially form in the absence of active cell movement. Mechanical models with a strong chemotactic element have particularly been studied for (*in vitro*) vasculogenesis (formation of the capillary network), and we refer to Ambrosi et al. (2005) for a review of this field.

The first detailed discussion of a “pure” PKS model in a developmental context was put forward for limb chondrogenesis. Limb development is mathematically appealing, featuring a bifurcation process in which modal transitions occur as the limb extends: for example, the arm bifurcates from the single humerus (upper arm) to the radius and ulna (forearm), before further bifurcations generate the hand and fingers. Oster and Murray (1989), suggested a simple model (C1) whereby chondroblasts secreted their own chemoattractant, discussing its merits with respect to generating realistic bifurcation sequences. Further analyses by Maini and others (Maini et al., 1991; Myerscough et al., 1998) extended to a quasi-2D cross section in which new

¹¹Father of modern neuroscience, and winner of the Nobel Prize in Medicine and Physiology in 1908.

¹²*Chemotropism* is more apt, as developing neurons grow (*-tropism*) rather than migrate: the neuron’s “growth cone” (a large cytoskeletal cell extension) migrates through the tissue and establishes the track of the lengthening axon.

bone is laid, explored heterogeneous steady states and their bifurcations and addressed the role of boundary conditions and tissue growth. Chemotaxis is certainly a plausible component of the chondrogenesis process – e.g. Mishima and Lotz (2008) – yet unsurprisingly it is significantly more complex: in fact, various studies suggest it may act as a melting-pot of various classic theories (e.g. positional information and Turing/RD ideas), see Green and Sharpe (2015). An obvious challenge for theoreticians is assessing the precise contributions of the various pattern generating mechanisms.

PKS models have been proposed in various other developmental processes, including pigmentation patterning of snakes (Murray and Myerscough, 1991) and fishes (Painter et al., 1999), gastrulation (Painter et al., 2000), neural crest invasion (Landman et al., 2003; Simpson et al., 2006), and feather morphogenesis (Michon et al., 2008; Lin et al., 2009; Painter et al., 2018). While the suggestion of chemotaxis was typically speculative at the time, it has since been placed on firmer biological foundations: e.g. during gastrulation (Yang et al., 2002) and neural crest invasion (Shellard and Mayor, 2016). Applications to feather formation, in particular, illustrate a closing gap between modelling and experiment with a number of integrated experimental/theoretical studies that utilise the PKS framework (Michon et al., 2008; Lin et al., 2009; Painter et al., 2018; Ho and Headon, In preparation). The model in Lin et al. (2009) was of standard PKS form (C1), featuring a population of chemotactic mesenchymal cells that regulate production of their attractant to generate the dermal cell aggregates at future feather sites. More detailed models have been proposed in Michon et al. (2008), where mesenchymal cells interact with a molecular network capable of pattern formation through Turing/activator-inhibitor instability (C2), and in Painter et al. (2018), where chemotactic-driven aggregation is generated mediated by epithelium signalling and molecular (FGF and BMP) regulators, model (C3). The capacity of these models to replicate feather placcode patterning and predict experimental perturbations offers a tantalising prospect for targeted future modelling.

7. Applications in physiology and disease

7.1. Background

Adult tissues and organs demand regeneration, monitoring and repair, invoking cell migration and chemotaxis amongst the numerous processes. The scope of this section limits us to a superficial coverage and we restrict to a few works of historical note. Reports of chemotactic responses in the immune system date to the late 19th century observations of Leber (1888) and Metchnikoff (1892)¹³, where phagocyte accumulation at infection sites was hypothesised to result from chemotactic guidance. Decades later, development of an *in vitro* assay in Boyden (1962) (the “Boyden chamber”) allowed (immune cell) chemotaxis to be studied quantitatively and reproducibly and a large family of *chemokines* (*chemotactic cytokines*, Griffith et al. 2014) are now known to control physiological chemotaxis, not just for immune system responses but many other processes. For example, during wound healing an assortment of chemokines act to guide cells from the early inflammation stage to final remodelling (Gillitzer and Goebeler, 2001).

The positive roles played by chemotaxis in defense and repair become ambiguous in disease. Inflammation couples tightly to many disease processes (Hunter, 2012), including in cancers, neurological diseases (e.g. multiple sclerosis, MS, and Alzheimer’s disease, AD), heart diseases (e.g. arteriosclerosis), diabetes, fibrosis *etc.* Inevitably, the question emerges as to whether “healthy” chemotactic processes become corrupted. Cancer is, quite obviously, of enormous interest and chemotaxis has been associated with numerous events, including angiogenic growth, invasion/metastasis of cancer cells and cancer-immune system interactions: see Roussos et al. (2011) for a review. Of course, unravelling the complex interactions and ascertaining whether a given chemotaxis event acts to delay or accelerate disease progress is far from trivial.

¹³Regarded as the founder of cellular immunology, and awarded the Nobel Prize in Medicine and Physiology in 1908.

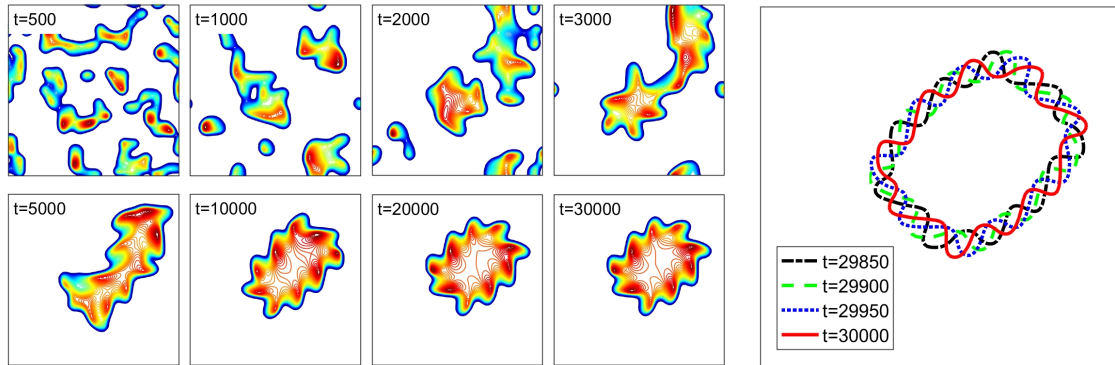


Figure 5: Evolution to a rotating star in the model (D4), with parameters set at $D_m = 0.45$, $D_c = 1$, $k_1 = 0.5$, $k_2 = 0.6$, $q = 1$, $k_3 = 50$ and $\chi = 2.8$. Left: cell densities (m) plotted at the times shown, with contour lines from dark blue to dark red indicating increasing density. Right: illustration of the rotating structure, with contour line for $m = 100$ plotted at four successive time points.

7.2. Modelling

Immune system dynamics have inspired volumes of models, with a number explicitly incorporating chemotaxis. Often, chemoattractant variables are discarded: for example, movement responses to bacteria infections can be modelled by assuming cells orient with respect to bacteria density gradients rather than explicit chemoattractants. Earliest PKS-based formulations were made by Lauffenburger and colleagues (Lauffenburger and Keller, 1979; Lauffenburger and Aris, 1979; Lauffenburger and Kennedy, 1983; Lauffenburger et al., 1984): in a patterning context, the model of Lauffenburger and Kennedy (1983) (see (D1)) demonstrated that a reduction in immune cell chemotaxis could lead to expansion and persistence of localised bacterial infections. Other PKS models for immune system dynamics include that in Lee et al. (2017), where patterning was investigated for immune cells responding to a foreign antigen, via chemokine-mediated chemotaxis (D2). In the context of viral infections, a spatial model of HIV dynamics was developed in Stancevic et al. (2013), where classic SIR dynamics were extended to incorporate chemotaxis. Specifically, uninfected “target” cells were attracted to virus-infected cells (and exposed to virus particles), see (D3), and the resulting model could generate spatial patterns representing infection “hot-spots”.

Skin rashes provide portraits of inflammations, and capturing their form has been the motivation of modelling studies dating to the reaction-diffusion approach of Segel et al. (1992). The acute inflammation model proposed in Penner et al. (2012) consisted of a generic immune cell population (e.g. macrophages) in the presence of a self-secreted chemokine and anti-inflammatory cytokine (D4). A raft of peculiar patterns were observed, such as the “rotating stars” shown in Figure 5. Vig and Wolgemuth (2014) specifically focussed on the rash *Erythema migrans*, an indicator of Lyme disease (transmitted via bacteria-infected tick bites). Their PKS model considered bacteria in stationary and motile forms and a population of chemotactic macrophages (D5) and replicated various clinical rash morphologies, along with predicting the impact of antibiotic treatment.

Inflammation events in neurodegenerative disorders, including MS and AD, have been investigated via a number of PKS models. The model in Luca et al. (2003) explored whether chemotactic microglia could be a driver in the formation of senile plaques, the lesions of proteins, degenerating neurons and glia cells that characterise AD. A combination of long range repulsion and short range attraction was shown to generate aggregates with the short wavelength clinical presentation. In Balós concentric sclerosis¹⁴, a pathological concentric ring pattern is generated as neurons lose their protective myelin sheaths (Figure 1f). A model

¹⁴A rare form of MS, where the brain’s oligodendrocytes are primary disease targets.

featuring chemotactic macrophages, a pro-inflammatory chemoattractant and oligodendrocytes (see (D7)) was shown to replicate these rings and offered a potential origin (Khonsari and Calvez, 2007); extensions and a more detailed pattern analysis were considered in Lombardo et al. (2017). A highly detailed model (D8) was developed in Silchenko and Tass (2015) to describe acute microglia responses, incorporating the interactions between microglia and attracting and/or repelling molecular substances (ATP, ADP, AMP and adenosine). Applied to the localised scarring generated at electrode implantation sites, the model generated stable aggregates and anti-scarring strategies were considered.

Angiogenesis has offered considerable modelling scope and a paragraph is insufficient to cover all contributions: several reviews cover these models in both tumour and wound induced angiogenesis (Mantzaris et al., 2004; Scianna et al., 2013; Flegg et al., 2015; Heck et al., 2015). Regarding pattern formation, the PKS model in Orme and Chaplain (1996) was of classic form (D9), featuring haptotactic-guided endothelial cells that respond to secreted fibronectin and initiate new sprouts along existing capillaries. Later models, such as Levine et al. (2001), greatly expanded the detail of cellular/molecular control. Other angiogenesis models have focussed on the wavelike extension of vessels in response to tumour angiogenic factors (TAFs). Of these, the “snail-trail” approach in Balding and McElwain (1985) (inspired by models for fungal networks, Edelstein 1982) has proven popular: capillaries are compartmentalised into separate tip/vessel variables (D11), with tip cells responding to TAF gradients and laying vessels as they migrate. Other early PKS-type models that focus on the extension of endothelial cells include that of Chaplain and Stuart (1993), featuring an attractant that diffuses (and degrades) from a boundary-source and an endothelial population that migrates and proliferates in response.

While they offer analytically tractable caricatures of the angiogenesis process, capturing the fine-scale structure of microvessels is difficult within coarsescale/continuous PKS models. Dating to fundamental studies of the 1990s (e.g. Stokes and Lauffenburger 1991; Anderson and Chaplain 1998), a large number of detailed agent-based/hybrid methods have been formulated, with their capacity to generate experimentally measurable outputs leading to a growing symbiosis between theory and experiment (see Bentley et al. 2013 for a review). The hybrid approach of Anderson and Chaplain (1998) is highlighted for its direct connection with PKS systems. Specifically, a continuous PKS-type system was proposed to describe tip cell densities (and other factors) and subsequently discretised in space to stipulate movement rules for an equivalent stochastic cellular automaton model. The capacity to generate realistic-looking network structure, as well as extend to include factors such as blood flow, has facilitated expansion of this approach and integration with experimental studies (Machado et al., 2011; McDougall et al., 2012). Fully continuous frameworks therefore remain a convenient method for formulating base models and ongoing work substantiates their link to underlying discrete processes, for example see Pillay et al. (2017) in the context of snail-trail concepts.

PKS models have been proposed in other aspects of tumour growth and, again, detailing all models would demand a separate review: we focus on those where spatial patterning emerges. The model in Owen and Sherratt (1997) investigated tumour-immune interplay, with macrophage chemotaxis in response to tumour-secreted factors (D12). A complex pattern of invasion was observed, including irregular spatio-temporal “tumour-clumps” that could generate heterogeneous invasion forms; the extension in d’Onofrio (2012) incorporated chemorepulsion in response to immune system effectors. Tumour-macrophage dynamics have also been the focus of Knútsdóttir et al. (2014), where interactions between tumour and macrophage populations (D13) were explicitly accounted for via a combination of “autotaxis” (taxis to a self-secreted chemical) and “parataxis” (taxis to a chemical secreted by a separate cell population) terms. Chaplain and Lolas (2006) developed a sequence of tumour invasion models (D14) that incorporated essential tumour/matrix interactions, with chemotaxis of tumour cells to uPA protease shown to induce complex/chaotic spatio-temporal clumping phenomena.

8. Applications in ecology

8.1. Background

Organisms frequently move in response to chemicals, self-evident from our reactions to enticing or noxious odours. Tracking dogs domesticated by our prehistoric ancestors reveal a long appreciation for animal senses (Morey, 1994) and Aristotle in the *History of Animals*¹⁵ recounts various stories, such as the use of repellents to disperse ants. Numerous orienteering paradigms have long been surmised to rely (partly) on odour sensing, including ant trail formation (Bonnet, 1779; Rennie, 1831), salmon homing (Trevanus, 1822) and moth mate location. Inspired by numerous male moths arriving at a room containing a captive female, 19th century naturalist Jean-Henri Fabre (1879, 1921) hypothesised her secretion of a powerful aroma. In one crucial experiment¹⁶, males ignored the visible female transferred to a new cage, attracted instead to the lingering smell of her previous perch. It is now firmly established that moths and many other species emit powerful pheromones that enable long-range communication.

Taxis responses are probable for many organisms: bilateral olfactory organs (antennae, forked tongues, nostrils) suggests instantaneous spatial gradients could, in principal, be detected. To varying certitude, chemotaxis has been proposed in soil nematodes (Lockery, 2011; Rasmann et al., 2012), the fruit fly *Drosophila melanogaster* in both larval (Gomez-Marin and Louis, 2012) and adult (Gaudry et al., 2012) stages, bees (Martin, 1965), snakes and other reptiles (Schwenk, 1994), moths and butterflies (Farkas and Shorey, 1972), various fish (Daghfous et al., 2012) including catfish (Johnsen and Teeter, 1980) and sharks (Mathewson and Hodgson, 1972), and lobsters (Reeder and Ache, 1980). Lack of certainty stems from the difficulty of precise tests: environments are complex, plumes subject to turbulence and contributions from other sensory inputs must be eliminated.

Our best understanding emerges in small organisms. Nematodes, such as *C. elegans*, have received particular interest and various chemoattractants have been identified (Ward, 1973). *C. elegans* climbs an attractant gradient via straight(ish) runs (generated by body undulations) alternating with “pirouettes” (reorientations). Analogous to *E. coli*, a similar klinokinesis behaviour has been identified in which pirouette frequency varies with the rate of concentration change (Pierce-Shimomura et al., 1999). Yet this is further augmented by klinotaxis: during undulations, the head swings side to side and small directional shifts occur according to the attractant gradient (Iino and Yoshida, 2009). Similar klinokinesis/klinotaxis combinations are suggested for larvae of the fruit fly *Drosophila melanogaster* (Gomez-Marin and Louis, 2012). An ability to orient directly to an instantaneous spatial gradient (tropotaxis) has been identified in adult *Drosophila*¹⁷ during both walking (Borst and Heisenberg, 1982) and flying (Duistermars et al., 2009): concentration differences are measured via the separated olfactory antennae. The extent to which this contributes to normal behaviour remains debatable, as other odour-following strategies exist such as flying upwind (anemotaxis) when an odour is sensed (Gomez-Marin and Louis, 2012). For mammals there are conflicting findings, although a body of work suggests rats (Rajan et al., 2006), and possibly even humans (Von Békésy, 1964; Porter et al., 2007), can ‘smell in stereo’: localising odours in a single sniff through the bilateral input provided by separated nostrils.

Self-organisation is widespread in ecology, with numerous species known to swarm, school, flock, herd *etc.* Chemically-mediated examples lead to social insects, such as ants and their capacity to generate intricate trail networks (Czaczkes et al., 2015), see Figure 1 (g). Briefly rubbing a finger across a trail can bring ants to a standstill, and 18th century zoologist Charles Bonnet (1779) surmised that ants used odours to

¹⁵An important translation was given by D’Arcy Wentworth Thompson, both pioneering mathematical biologist and highly-regarded classicist (Aristotle, 1907).

¹⁶In the course of his experiments, Fabre learned why you should not place a rare specimen in a tank containing a preying mantis. The moth bore the brunt of the error.

¹⁷Chemotaxis in fruit flies was investigated much earlier (Severin and Severin, 1914), exploring Kerosene as a trap for the Mediterranean Fruit Fly *Ceratitis capitata*. However, this species derives from a completely different family of fruit flies.

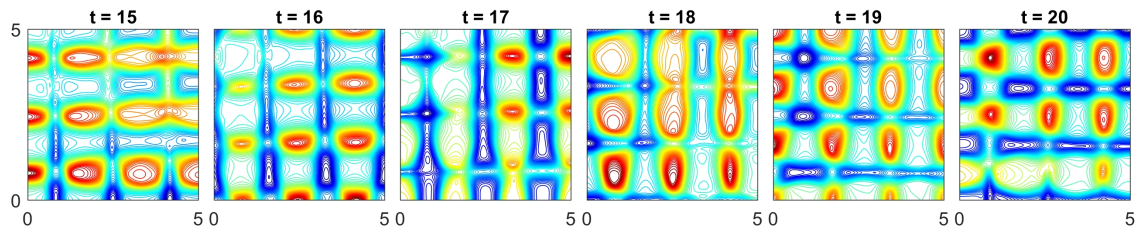


Figure 6: Oscillating patterns in the forager-scrounger model (E2). Frames show forager density, with contour lines blue to red reflecting increasing density. Parameters set at $D_f = D_s = 1$, $D_r = 0.1$, $\chi_f = \chi_s = 10$, $G = H = 0$ and $k_1 = 8.05, k_2 = 8, k_3 = 0.05$. The population is equally composed between foragers and scroungers.

mark the route. The modern view developed from findings of the 1960s: Wilson (1962) showed that the different pheromone trails at a nest would recruit ants according to their concentration, while Hangartner (1967, 1969) showed that branch selection was proportional to its pheromone concentration and that ants release more pheromone if the food source is of higher quality. This suggested a powerful feedback process in which trails leading to the best sites are most strongly signalled, allowing the colony to efficiently harvest its surroundings (for a general review, see Czaczkes et al. 2015). Further examples of chemically-mediated group aggregation can be found in species such as tent caterpillars (Fitzgerald and Costa, 1999).

8.2. Modelling

PKS terms incorporated within ecological models are often phenomenologically motivated, for example “preytaxis” fluxes to model predator movement responses to a prey distribution (Kareiva and Odell, 1987). Incorporating preytaxis into biological invasion models suggests it can potentially accelerate invasion, by drawing predators away from the leading edge and giving outlying prey a greater survival chance (Lee et al., 2008). In the context of pattern formation prey-taxis acts to stabilise, shifting the system towards spatial uniformity rather than group-forming behaviour (Lee et al., 2009): intuitively, predators diminish their attractor (the prey) rather than reinforcing it. An intriguing extension, though, has been suggested in Tania et al. (2012) where a PKS model (E2) was used to describe “forager/scrounger” systems. Here, the forager (predator) searches for food (prey), modelled via food gradient following. The scrounger instead exploits the efforts of the forager, following the forager gradient rather than actively seeking its own food: interactions of this kind are observed, for example, in certain seabird populations. Surprisingly, the seemingly innocuous addition of scrounging can act as a destabiliser, breaking homogeneity to generate temporally-oscillating spatial patterns (Figure 6).

PKS models have also been proposed for specific ecological systems. Pearce et al. (2007) developed a multi-species host-parasitoid system (E3), including two parasitoid wasps, their hosts (caterpillars of the large and small cabbage white butterflies) and a chemical secreted by feeding hosts. Wasps attracted by this factor accumulate at feeding sites, with sufficiently powerful responses inducing spatially structured, potentially chaotic, distributions. PKS models have also been applied to describe ant trail formation (Ramakrishnan et al., 2014; Amorim, 2015), with chemotaxis used to describe pheromone trail following by foraging ants (E4,E5). Pheromone-mediated movement has been added into various models of mountain pine beetle infestation, a destructive species that exploits (and kills) trees during its reproduction. Successful attacks demand pine beetle accumulation, coordinated via their secretion of powerful aggregation-inducing pheromones. A detailed PKS-type model (E6) described airborne and nesting beetles, their secreted pheromones, the density of tree attack holes for colonising beetles, chemicals (kairomones) released by host trees and the tree’s resin capacity/outflow rate, see Powell et al. (1996). While the dynamics of initial outbreaks were shown to be determined by the distribution of host trees, later dynamics were governed by the aggregation-inducing

process of pheromone secretion/attraction (Logan et al., 1998). A reduced version of the model (E6), featuring nesting and flying beetles and the aggregation pheromone, has been analysed in Powell et al. (1998) and Strohm et al. (2013).

9. Applications in the social sciences

Core applications of PKS models obviously rest in biology, but we conclude the review component with a brief digression into the social sciences. Taxis responses here are highly phenomenological, capturing some broad behaviour rather than a specific movement response to a chemical gradient. For example, a PKS model developed in Neto and Claeysen (2015) was framed within an economic setting, addressing the interaction between “capital” and “labour” in economies: in essence, greater labour generates more capital and capital attracts labour, the latter explicitly modelled via a PKS-taxis flux of labour towards capital. The resulting model, see (F1), was used to show how labour and capital co-localise and form dominating economies, as well as the potential for complex and unpredictable temporal behaviour to arise.

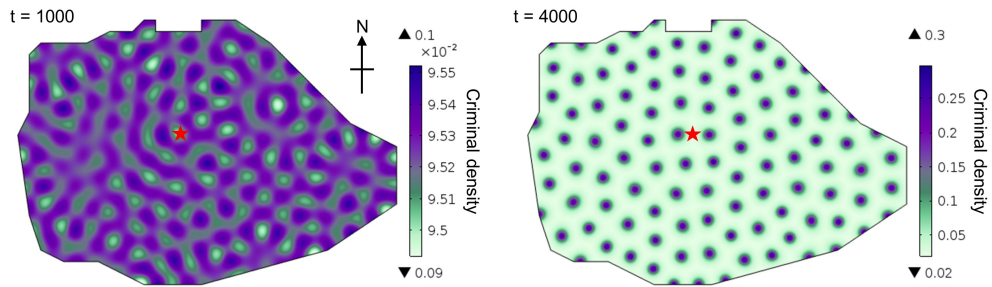


Figure 7: Crime hotspot model (F2), where criminal density is plotted at $t = 1000$ and $t = 4000$ (green to purple reflects increasing criminal density) and parameters are set at $k_1 = 0.05$, $k_2 = 0.5$, $k_3 = 0.05$, $D_c = 100$, $D_a = 2$ and $b = 0.025$. Here, equations have been solved on a spatial region approximately describing the outline of Edinburgh (red star reflects the position of Edinburgh Castle).

Crime modelling has received significant interest and statistical analyses of criminal data reveal spatio-temporal structuring such as transient or long-lasting “hotspots” of elevated activity. Short et al. (2008, 2010b) sought to explore how these hotspots arise. An agent-based model was proposed for residential crime activity, based on “repeat-victimisation” and “broken-windows” phenomena: burgled properties and their neighbours are statistically likely to suffer repeat attack in a period following a crime. Mobile criminal agents responded to an “attractiveness” field, representing the desirability of properties. In a continuous limit a PKS-type model (F2) was obtained for criminal density and the attractiveness field, with biased movement towards attractive locations generating the taxis term. Crimes were committed at a rate according to local attractiveness, modifying this field both locally (repeat-victimisation) and nearby (broken-windows) in the process. The resulting model had the essential structure of an autotaxis system, so that spatial pattern (corresponding to hotspots) could occur even under initially homogeneous attractiveness (see Figure 7): hotspots can emerge in cities without historically “bad neighbourhoods”. While the concept of attractiveness is obviously difficult to quantify, the model successfully shows how the empirical observations can lead to complex spatial structuring and provides a means for exploring effective deployment of anti-crime measures. Various extensions have been considered (Short et al., 2010a; Jones et al., 2010; Short et al., 2010b; Pitcher, 2010; Zipkin et al., 2014; Gu et al., 2017), in particular to include policing (as one example, see model (F3)) and we refer to D’Orsogna and Perc (2015) for a review of this developing field.

10. Academic clique formation

The above sections reveal a widening usage of PKS equations, and we conclude with a light-hearted and novel case study. Specifically, we formulate a model for *research drift*, defined as the tendency of academics to alter their line of research over time. We show that biased drift according to perceived problems can generate an *academic clique* (a cluster of researchers working on the same topic) and “hot” research topics. The number of mathematicians currently analysing chemotaxis models would appear to be an apt example.

10.1. Model equations

We develop a model for the rate of change of academics, $a(\mathbf{x}, t)$, at time t . Here, $\mathbf{x} \in \Omega$ is not position in standard three-dimensional space, but a specific *line of research* in some *research field* Ω . We assume \mathbf{x} is a continuous real variable, i.e. $\mathbf{x} \in \Omega \subset \mathbb{R}^n$: if mathematical biology was the research field, modelling tumour invasion or angiogenesis could be regarded as two separate, but close, points in Ω ¹⁸. We assume academics can do two things¹⁹:

- (S1) solve problems;
- (S2) change their line of research over time (research drift);

Supposition (S1) implies that the number of problems is an important variable: if all problems are solved there is no point doing research. Of course, problems are of varying difficulty²⁰ and, to account for this variation, we compartmentalise problems into harder ($h(\mathbf{x}, t)$) and easier ($e(\mathbf{x}, t)$) problems. (S2) implies a movement flux in which academics move through their research field. Following classical conservation arguments,

$$\frac{\partial a}{\partial t} = -\nabla \cdot \mathbf{J}_a + f(\cdot),$$

where flux $\mathbf{J}_a(\mathbf{x}, t)$ describes research drift and f is the population change. We assume any movement is local – a nonlocal (e.g. integral) formulation could allow scholars to radically change research, but we discount this at present. Research drift is assumed to derive from: (i) a random component; (ii) directed components towards areas with many identifiable problems²¹. The former describes “chance encounters” in a nearby topic (e.g. inspired by a chance-found paper), while the latter accounts for actively seeking areas with questions to solve (e.g. noting hot topics at conferences). The function f is likely to be non-zero, since researchers can enter (PhD students...) or exit (retiring or moving into university management...). Generally, f would depend on both the number of academics and problems: problems to solve implies papers to write implies grant success implies new students; no more problems, and academics may exit research. Taken together, we assume the following PKS equation for $a(\mathbf{x}, t)$:

$$\frac{\partial a}{\partial t} = \nabla \cdot [D\nabla a - \chi_e a \nabla e - \chi_h a \nabla h] + f(a, h, e). \quad (2)$$

D, χ_e and χ_h are likely to be functions of both the number of academics and number of problems, however for simplicity we shall set them to be constants. $\chi_{e,h}$ are measures of attraction towards problems and how rapidly a research line can be altered.

Problem variables are governed by the following factors:

- (S3) problems are solved at a rate that increases with the number of academics;
- (S4) solving one problem can create further problems;

¹⁸At its most general Ω would cover the full spectrum of academic disciplines (maths, physics, biology, humanities, social sciences etc) and is therefore of high dimensionality. This validates any theoretical attempts to prove results for dimensions > 3 ...

¹⁹Insert a joke here...

²⁰Showing $a^n + b^n = c^n$ ($a, b, c, n \in \mathbb{Z}$) has no solutions for $n > 2$ was considerably harder than showing it does for $n = 2$...

²¹“Problemataxis”

(S5) problems “transfer” to nearby areas.

(S3) follows a “more hands make light work” presumption: problems will be solved more quickly if more academics work in the area. (S4) presumes that solving one problem can lead to new ones, e.g. questions raised in the discussion of a paper/conclusions of a talk. (S5) accounts for how questions raised in one field can generate a similar question in a nearby area. Here, we set

$$\frac{\partial e}{\partial t} = D_e \nabla^2 e - g_e(a)e + \gamma_{eh}g_h(a)h + \gamma_{ee}g_e(a)e - \delta_e e, \quad (3)$$

$$\frac{\partial h}{\partial t} = D_h \nabla^2 h - g_h(a)h + \gamma_{hh}g_h(a)h + \gamma_{he}g_e(a)e - \delta_h h. \quad (4)$$

We note that “transfer” has been modelled simplistically here, via diffusion terms, although (S5) more accurately suggests problem creation in adjacent areas. Problems are solved at rates $g_i(a)$, $i \in \{e, h\}$, and solving a problem of type j is assumed to create γ_{ij} new problems of type i . The linear decay terms account for raised problems being “forgotten”: e.g. nobody reads the discussion :-)

10.2. Functions and parameter constraints

We solve (2-4) under choices $f = 0$ and $g_i = \frac{\alpha_i a}{1 + \kappa_i a}$ for $i \in \{e, h\}$. The simplification $f = 0$ presumes a population of *selfish immortal academics*: they never retire, never move into administration and never supervise new students²². The choice of g 's assumes problems are solved at a rate that increases, but eventually saturates, with the number of academics: a “law of diminishing returns”, where increasing numbers leads to overlapping work and proportionally lower rate gain of problem solving.

Parameter restrictions are motivated by the following set of considerations.

- (P1) $\chi_e > \chi_h$. Academics are more attracted to areas with easier problems. This reflects two factors: (i) “publish or perish”, where quickly solving problems (and hence publishing) is considered the best method for rapid career progression; (ii) harder problems are difficult to identify. We specifically set $\chi_h = 0$ here.
- (P2) $\alpha_e \gg \alpha_h > 0$. The maximum rate of solving easier problems is significantly faster than solving hard problems, although the latter is nonzero.
- (P3) $\delta_e \gg \delta_h$. Easier problems are far more likely to be forgotten than harder problems: ‘Fermat’s last theorem was remembered more than three centuries later, but no-one remember the problem I posed during the talk at XXXX last year’. We specifically set $\delta_h = 0$ here.
- (P4) $\gamma_{eh} \gg \gamma_{hh}, \gamma_{ee}, \gamma_{he}$. In other words, solving a hard problem can generate lots of easy problems: devising a new analytical/experimental technique that can be adopted for similar problems. We specifically consider $\gamma_{eh} > 0$ and $\gamma_{hh} = \gamma_{ee} = \gamma_{he} = 0$ here.

Initially we suppose academics are uniformly distributed across the field, $a(\mathbf{x}, 0) = a_0$, so that there is no initial clustering. We further start with hard problems only: easy problems only emerge when some hard problems are solved. Thus, we take $e(\mathbf{x}, 0) = 0$ and set $h(\mathbf{x}, 0) = h_0(1 + r(\mathbf{x}, 0))$ where $r(\mathbf{x}, t) \in [-0.01, 0.01]$ represents a small random variable. At boundaries we impose zero-flux conditions for both the academics and problems: i.e. neither can exit their research field²³.

10.3. Dynamics and clustering

We solve (2-4) subject to the functions, parameter constraints, initial and boundary conditions above. Note that for simplicity we restrict the academic field to a one dimensional line $[0, L]$; points 0 and L can be interpreted as the most distantly related topics in a research field. For low values of χ_e (academics do not

²²Many academics may want this. More charitably, $f = 0$ implies each exiting academic is replaced by one new researcher.

²³Polymaths of the past, such as D’Arcy Wentworth Thompson, are taken to be rare.

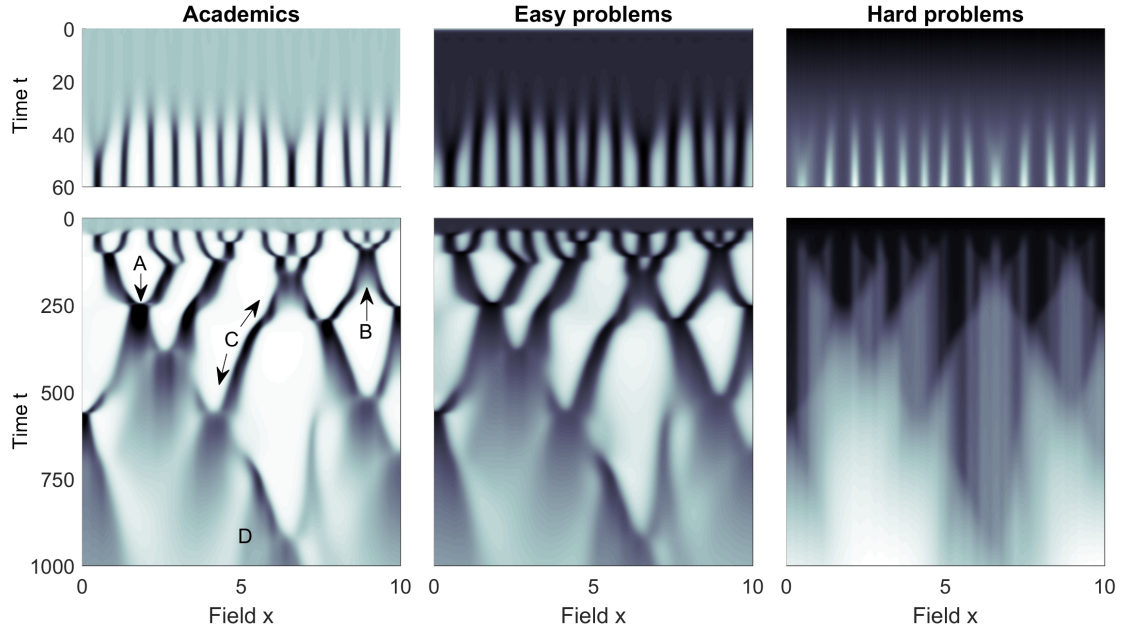


Figure 8: Simulations of the research drift model (equations (2-4)), with functions and parameter constraints as described in the text. Grayscale from white to black represents increasing density of academics or problems. Top row: incipient stages of pattern formation, where an initially uniform distribution of academics self-organise into distinct “cliques” as progress is made on solving problems. Bottom row: spatio-temporal dynamics over longer timescales, with dynamics showing: (A) convergence; (B) divergence; (C) clique drift; and (D) eventual field death. In these simulations we set $D_A = D_E = 0.01, D_H = 0, \chi_E = 0.1, \chi_H = 0, \alpha_e = 1, \alpha_h = 0.001, \kappa_h = 0.1, \kappa_e = 0.01, \gamma_{eh} = 1, \gamma_{hh} = \gamma_{ee} = \gamma_{he} = 0$.

tend to alter their research according to problems), no patterning emerges and the distribution of scholars remains uniform. For larger values, however, a self-organisation process occurs with typical simulations shown in Figure 8 for (a) shorter, and (b) longer timescales. Briefly, the underlying randomness leads to a variable rate of progress at solving hard problems. Solving harder problems, however, then creates numerous easier problems and fuels a “gold-rush” of eager academics from nearby areas. This in turn quickens the rate at which harder problems are solved, reinforcing the process. Thus, we have the essential feedback for taxis-based self-organisation.

Over longer timescales we observe more complicated phenomena as follows.

- (A) Research convergence, where closely related groups “join forces” and start working on a common topic.
- (B) Research divergence, where a group splits into separate research lines.
- (C) Group drifting, where a group of academics steadily shifts its line of research as it searches for new problems to work on.
- (D) Field death. Eventually, all problems are solved and clusters disperse.

11. Perspectives

More than a century has passed since the earliest identification of chemotaxis, and more than half a century since their first mathematical models. In the following years a vast literature has developed, and chemotactic behaviour has been incorporated into numerous models to address numerous questions in numerous fields. Moreover, a large mathematical literature has emerged, leading to an elegant understanding of their

mathematical properties. As of late 2017, the first paper of Keller and Segel (1970) has attracted more than 2,000 citations (Google Scholar).

At what point does a model stop being useful? Paraphrasing Mae West²⁴, a model's just an imitation of real life so the obvious answer is when it fails to imitate. Inevitably, this depends on the problem being addressed, but, in all discussed areas, recent applications have been made of the PKS framework. This certainly suggests their ongoing relevance but it is noted that for the vast majority of studies, model *fitting* has generally been performed at a qualitative or semi-quantitative level. As data becomes increasingly nuanced, more stringent tests must be made via carefully constructed quantitative comparisons: in this regard the recent study of Ferguson et al. (2016) provides a promising start.

Molecular/individual-scale understanding has advanced considerably and, with parallel advances in computational power, modelling has evolved via agent-based approaches and their ilk. These have proven enormously appealing, admitting intricate and tailored detail that connects easily to biological data: unsurprisingly, all applications considered have witnessed significant modelling of this nature. Nevertheless, these approaches rely heavily on computation while continuous models can admit deeper analysis and broader-scale enlightenment. Keeping pace with these individual models, however, will demand that continuous models evolve to import key microscopic elements. For example, phenomena such as "collective chemotaxis" (Theveneau et al., 2010), where clusters performs chemotaxis more efficiently than isolated cells, appears to fundamentally depend on microscale interactions between cells: can appropriate PKS-type models be derived to describe these phenomena? Other areas for fundamental modelling include accounting for cell polarization or heterogeneous populations, where two or more populations exist with distinct movement properties. In terms of the latter, one approach (taken by several models in the compendium) is to simply include multiple populations with standard fluxes. This may be reasonable at relatively low densities, but in tightly packed populations (e.g. spore/stalk cells in the slug), movement of one population could clearly influence the other. A number of attempts have been made to model such behaviour, e.g. Painter and Sherratt (2003); Painter (2009); Simpson et al. (2009); Johnston et al. (2015).

The number of recent applications, particularly in areas such as ecology and the social sciences, suggests that the well of problems is far from dry. Indeed, its limits may rest only in our imagination and, to illustrate, we have considered a novel application in the social sciences. Taxis here is a hazier concept, and the broad nature of PKS-type fluxes is an attractive way of characterising the essence of a phenomena. While our model has been constructed in a somewhat playful manner, there is obvious interest in the positives and negative implications of social group formation: not just academically, but school or office cliques, political opinion, groupthink, religious circles, social networking sites *etc.* (Backstrom et al., 2006). For example, the ideas here could be adapted to explore the drivers of extremism, for a population structured according to opinion and fluxes driving shifting political thought.

Our modelling provides an intuitive explanation for how academic cliques form: progress on harder problems leads to easier problems, attracting scholars. Progress quickens and so forth. Over time, various phenomena emerge including the convergence and divergence of groups or group drifting across the research field. Our principal aim has been demonstrative, but various factors could warrant greater analysis: including nonzero kinetics to account for incoming PhD students *etc.*; population heterogeneity (e.g. "lone wolf" academics that avoid crowded areas); including the impact from measurable factors such as research funding and publications *etc.*

In our model, the number of problems, eventually, runs dry. Research clustering disappears and the field dies. In a population of selfish immortal academics, they disperse and are condemned to an eternity of writing review articles.

Acknowledgements. KJP would like to thank the Politecnico di Torino for a Visiting Professorship position, Thomas Hillen for highly constructive comments and Philip Maini for originally introducing him to the subject.

²⁴"I'm no model lady, a model's just an imitation of the real thing".

Appendix A. A compendium of PKS models for pattern formation

Note that in the following we generally use D_i 's to denote diffusion coefficients, χ_i 's to denote chemotactic sensitivity coefficients and k_i 's as constants. We refer to the original articles for full details and model motivations.

Appendix A.1. Models for Dd aggregation

Keller and Segel (1970) model for *Dd* aggregation, for densities of amoebae (a), concentrations of acrasin (c), acrasinase (p) and complex (q):

$$\begin{aligned} a_t &= \nabla \cdot [D_a \nabla a - a\chi(a, c)\nabla c], \\ c_t &= D_c \nabla^2 c + aF(c) + k_2 q - k_1 c p, \\ q_t &= D_q \nabla^2 q + k_1 c p - (k_2 + k_3)q, \\ p_t &= D_p \nabla^2 p + (k_2 + k_3)q + aG(c, p) - k_1 p c. \end{aligned} \quad (\text{A1})$$

Reduced (two variable) version:

$$\begin{aligned} a_t &= \nabla \cdot [D_a \nabla a - a\chi(a, c)\nabla c], \\ c_t &= D_c \nabla^2 c + aF(c) - H(c)c. \end{aligned} \quad (\text{A2})$$

Hofer et al. (1995) model for *Dd* aggregation, for cells (n), cAMP concentration (u) and fraction of active cAMP receptors (v):

$$\begin{aligned} n_t &= \nabla \cdot \left[D_n \nabla n - \chi_0 \frac{nv^m}{k_3 + v^m} \nabla u \right], \\ u_t &= D_u \nabla^2 u + k_1 (G(n)F(u, v)) - (G(n) + k_2)k_6 u, \\ v_t &= -k_9 uv + k_{10}(1 - v), \end{aligned} \quad (\text{A3})$$

where $F(u, v) = (k_4 v + v^2)(k_5 + u^2)/(1 + u^2)$, $G(n) = n/(1 - k_7 n/(k_8 + n))$.

Appendix A.2. Models for bacteria pattern formation

Woodward et al. (1995) model for salmonella pattern formation, for bacteria density (u) and aspartate (v):

$$\begin{aligned} u_t &= \nabla \cdot \left[D_u \nabla u - \frac{\chi u}{(1+k_1 v)^2} \nabla v \right] + k_2 u \left(1 - \frac{u}{s} \right), \\ v_t &= D_v \nabla^2 v + \frac{k_3 s u}{1+k_4 u} - \frac{k_5 v u^p}{1+k_6 v}. \end{aligned} \quad (\text{B1})$$

Note that s represents a (constant) nutrient source.

Tsimring et al. (1995) model for bacteria pattern formation, for motile bacteria (m), non-motile bacteria (n), nutrient (f), waste product (w), chemoattractant (c):

$$\begin{aligned} m_t &= \nabla \cdot [D_m \nabla m - \chi m \nabla c] + k_1 m^p \frac{f}{f+k_2} - m^3 - H_1(\cdot)m, \\ n_t &= H_1(\cdot)m, \\ f_t &= D_f \nabla^2 f - k_3 m f, \\ w_t &= D_w \nabla^2 w + k_4 m f - k_5 w - k_6 m w, \\ c_t &= D_c \nabla^2 c + H_2(\cdot)m - k_7 c. \end{aligned} \quad (\text{B2})$$

Functions $H_1(\cdot)$ and $H_2(\cdot)$ are based on Heaviside functions, respectively describing the switching to non-motile form as starvation occurs and chemoattractant secretion according to the waste product.

Tyson et al. (1999a) model for bacteria pattern formation, for bacteria (n), nutrient (succinate, s) and chemoattractant (aspartate, c):

$$\begin{aligned} n_t &= \nabla \cdot \left[D_n \nabla n - \frac{\chi n}{(k_1+c)^2} \nabla c \right] + k_2 n \left(\frac{k_3 s^2}{k_4+s^2} - n \right), \\ c_t &= D_c \nabla^2 c + k_5 s \frac{n^2}{k_6+n^2} - k_7 n c, \\ s_t &= D_s \nabla^2 s - k_8 n \frac{k_3 s^2}{k_4+s^2}. \end{aligned} \quad (\text{B3})$$

Polezhaev et al. (2006) model for bacteria pattern formation, for vegetative bacteria (n), antibiotic bacteria (a), chemoattractant (c) and nutrient (s):

$$\begin{aligned} n_t &= \nabla \cdot \left[D_n \nabla n - n \frac{\chi}{(c+k_1)^2} \nabla c \right] + \frac{k_2 s}{s+k_3} n - k_4 n H(n) H(n+a-k_5), \\ a_t &= k_4 n H(n) H(n+a-k_5), \\ c_t &= D_c \nabla^2 c + A(s) n - k_6 c, \\ s_t &= D_s \nabla^2 s - \frac{k_2 s}{s+k_3} n, \end{aligned} \quad (\text{B4})$$

where $A(s) = \begin{cases} k_7 s, & s \geq k_8 \\ k_7 k_8, & s < k_8 \end{cases}$ and $H(\cdot)$ represents the Heaviside function.

Aotani et al. (2010) model for bacteria pattern formation, for active cells (u), inactive cells (w), chemoattractant (c) and nutrient (n):

$$\begin{aligned} u_t &= \nabla \cdot \left[D_u \nabla u - u \nabla \frac{\chi_0 c^2}{c^2+k_1^2} \right] + g(u) n u - \frac{k_4}{k_5+n} u, \\ c_t &= D_c \nabla^2 c + k_6 u - k_7 c, \\ n_t &= D_n \nabla^2 n - k_8 g(u) n u, \\ w_t &= \frac{k_4}{k_5+n} u, \end{aligned} \quad (\text{B5})$$

for $g(u) = (1 + \tanh(k_2(u - k_3)))/2$.

Baronas et al. (2015) for *E. coli* pattern formation, for bacteria (n), nutrient (succinate, s) and chemoattractant (aspartate, c):

$$\begin{aligned} n_t &= \nabla \cdot [D_n \nabla n - \chi n \nabla c] + k_1 n (1 - n/k_2 s), \\ c_t &= D_c \nabla^2 c + \frac{k_3 n}{k_4+n} - k_5 c, \\ s_t &= D_s \nabla^2 s - k_6 n. \end{aligned} \quad (\text{B6})$$

Chemotaxis-fluid models (Hillesdon et al., 1995; Tuval et al., 2005; Chertock et al., 2012)) for *B. subtilis* pattern formation in thin fluid layers, for bacteria (n), oxygen (o) and fluid velocity vector field (\mathbf{u}):

$$\begin{aligned} n_t + \mathbf{u} \cdot \nabla n &= \nabla \cdot [D_n \nabla n - \chi(o) n \nabla o], \\ o_t + \mathbf{u} \cdot \nabla o &= D_o \nabla^2 o - k_1 n F(o), \\ \rho(\mathbf{u}_t + \mathbf{u} \cdot \nabla \mathbf{u}) &= -\nabla p + \eta \nabla^2 \mathbf{u} - n \nabla G, \end{aligned} \quad (\text{B8})$$

and $\nabla \cdot \mathbf{u} = 0$, with pressure p and viscosity η . Gravitational force is modelled by $\nabla G = V_b g \mathbf{z} (\rho_b - \rho)$, where \mathbf{z} is the downward unit vector, V_b is the volume of the bacteria and ρ, ρ_b are respectively fluid and bacteria densities.

Appendix A.3. Models for embryogenesis

Chemotaxis model applied to embryonic pattern formation in chondrogenesis (Oster and Murray, 1989; Maini et al., 1991; Myerscough et al., 1998), snake pigmentation (Murray and Myerscough, 1991) and feather morphogenesis (Lin et al., 2009). Cells (n) and chemoattractant (c):

$$\begin{aligned} n_t &= \nabla \cdot [D_n \nabla n - \chi n \nabla c] + k_1 n (k_2 - n), \\ c_t &= D_c \nabla^2 c + \frac{k_3 n}{k_4+n} - k_5 c. \end{aligned} \quad (\text{C1})$$

Michon et al. (2008) model for feather morphogenesis, for proliferating (n) and migrating (m) mesenchymal cells, activator chemoattractant (u) and inhibitor (v):

$$\begin{aligned} n_t &= \begin{cases} k_1 n(k_2 - n) & t \leq t^* \\ -k_3 n & t > t^* \end{cases} \\ m_t &= \nabla \cdot [D_m \nabla m - \chi m \nabla u] + \begin{cases} 0 & t \leq t^* \\ k_3 n & t > t^* \end{cases}, \\ u_t &= D_u \nabla^2 u + \frac{k_4 m(1+k_5 u^2)}{(k_6+u^2)(1+v)} - k_7 u, \\ v_t &= D_v \nabla^2 v + k_8 m u^2 - k_9 v. \end{aligned} \quad (C2)$$

Painter et al. (2018) model for feather morphogenesis, for mesenchymal cells (m), activated epithelial (e), FGF (f) and BMP (b),

$$\begin{aligned} m_t &= \nabla \cdot [D_m \nabla m - \chi m e^{-k_1 m} \nabla f], \\ e_t &= (k_2 W(x, y, t) G_1(m) + k_2 G_2(m))(1 - e) - (1 - G_1(m))(k_3 + k_4 b) e, \\ f_t &= D_f \nabla^2 f + k_5 e - k_6 f, \\ b_t &= D_b \nabla^2 b + k_7 G_3(m) m - k_8 b, \end{aligned} \quad (C3)$$

with priming wave $W(x, y, t) = k_9(1 + \tanh(k_{10}(t - y/k_{11})))$ and $G_i(m) = m^{p_i} / (k_i^{p_i} + m^{p_i})$.

Appendix A.4. Models in physiology and disease

Lauffenburger and Kennedy (1983) model for tissue inflammation responses to infection, for a bacteria population (b) and phagocytising immune cells (p):

$$\begin{aligned} p_t &= \nabla \cdot [D_p \nabla p - \chi p \nabla b] + k_1 + k_2 b - k_3 p, \\ b_t &= D_b \nabla b + \frac{k_4 b}{k_5 + b} - \frac{k_6 b p}{k_7 + b}. \end{aligned} \quad (D1)$$

Lee et al. (2017) model for active immune cells (m), antigen (a) and chemokines (c):

$$\begin{aligned} m_t &= \nabla \cdot [D_m \nabla m - \chi(c) m \nabla c] + k_1 - k_2 m a - k_3 m, \\ a_t &= D_a \nabla^2 a + s(t, x) - k_3 m a - k_4 a, \\ c_t &= D_c \nabla^2 c + k_5 m a - k_6 c. \end{aligned} \quad (D2)$$

Note that $s(t, x)$ represents an antigen source (spatially localised).

Stancevic et al. (2013) model for HIV infection spatial dynamics, for target cells (n), infected cells (i) and virus (v):

$$\begin{aligned} n_t &= \nabla \cdot [D_n \nabla n - \chi(n) n \nabla i] + k_1 - k_2 n v - k_3 n, \\ i_t &= D_i \nabla^2 i + k_2 n v - k_4 i, \\ v_t &= D_v \nabla^2 v + k_5 i - k_6 v. \end{aligned} \quad (D3)$$

Penner et al. (2012) model for tissue inflammation, applied to skin rashes, for macrophages (m), a chemokine (c) and anti-cytokine (a):

$$\begin{aligned} m_t &= \nabla \cdot [D_m \nabla m - \frac{\chi m}{(1+k_1 c)^2} \nabla c], \\ c_t &= D_c \nabla^2 c + \frac{m}{1+k_2 a^q} - c, \\ a_t &= \frac{1}{k_3} (D_c \nabla^2 a + \frac{m}{1+k_2 a^q} - a). \end{aligned} \quad (D4)$$

Vig and Wolgemuth (2014) model for *Erythema Migrans*, for macrophages (m), translocating bacteria (b) and stationary bacteria (s):

$$\begin{aligned} m_t &= -\nabla \cdot [\chi m \nabla (b + s)] + k_1 (b + s) - k_2 m, \\ b_t &= D_b \nabla^2 b + k_3 b + k_4 s - k_5 b - k_6 m b, \\ s_t &= k_3 s - k_4 s + k_5 b - k_7 m s. \end{aligned} \quad (D5)$$

Luca et al. (2003) model for plaque formation in AD, for microglia (m) and regulatory chemicals (b, c):

$$\begin{aligned} m_t &= \nabla \cdot [D_m \nabla m - \chi_b m \nabla b + \chi_c m \nabla c], \\ b_t &= D_b \nabla^2 b + k_1 m - k_2 b, \\ c_t &= D_c \nabla^2 c + k_3 m - k_4 c. \end{aligned} \quad (D6)$$

Khonsari and Calvez (2007) and Lombardo et al. (2017) model for Balós concentric sclerosis, for macrophages (m), oligodendrocytes (d) and chemoattractant (c):

$$\begin{aligned} m_t &= \nabla \cdot [D_m \nabla m - \chi(m) \nabla c] + k_1 m (k_2 - m), \\ k_3 c_t &= D_c \nabla^2 c + k_4 d + k_5 m - k_6 c, \\ d_t &= \frac{k_7 m}{k_2 + m} m (k_8 - d). \end{aligned} \quad (D7)$$

Note that $\chi(m) = \chi_0 m (k_2 - m)$ in Khonsari and Calvez (2007) and $\chi(m) = \chi_0 \frac{m}{k_2 + m}$ in Lombardo et al. (2017); $k_3 = k_5 = 0$ in Khonsari and Calvez (2007).

Silchenko and Tass (2015) model for microglia aggregation, for microglia (n), and concentrations of ATP (a), ADP (b), AMP (c) and adenosine (d) and IL-1 (e):

$$\begin{aligned} n_t &= \nabla \cdot \left[D_n \nabla n - \frac{\chi_1 n}{(k_1 + a)^2} \nabla a - \frac{\chi_2 n}{(k_2 + b)^2} \nabla b - n \chi_3 F(d) \nabla d + n \chi_4 \nabla e \right], \\ a_t &= D_a \nabla^2 a + k_3 n + \frac{k_4 a}{a + k_5} - \frac{k_6 a}{a + k_7} - \frac{k_8 a}{a + k_9}, \\ b_t &= D_b \nabla^2 b + \frac{k_6 a}{a + k_7} - \frac{k_{10} b}{b + k_{11}}, \\ c_t &= D_c \nabla^2 c + \frac{k_{10} b}{b + k_{11}} + \frac{k_8 a}{a + k_9} - \frac{k_{12} c}{c + k_{13}(1 + k_{14} b)}, \\ d_t &= D_d \nabla^2 d + \frac{k_{12} c}{c + k_{13}(1 + k_{14} b)} - \frac{k_{15} d}{d + k_{16}}, \\ e_t &= D_e \nabla^2 e - k_{17} e + k_{18} n + k_{19}. \end{aligned} \quad (D8)$$

Note that $F(d) = (k_{20} - k_{21} d^2) / (k_{22}^2 + d^2)$.

Orme and Chaplain (1996) model for capillary sprout initiation, for endothelial cells (n) and fibronectin (c):

$$\begin{aligned} n_t &= \nabla \cdot [D_n \nabla n - \chi n \nabla c] + k_1 n (k_2 - n), \\ c_t &= D_c \nabla^2 c + \frac{k_3 n}{k_4 + n} - k_5 c. \end{aligned} \quad (D9)$$

Orme and Chaplain (1996) model for capillary branching, for endothelial cells (n), matrix density (r) and adhesion sites (a):

$$\begin{aligned} n_t &= \nabla \cdot [D_n \nabla n - \chi_1 n \nabla a + \chi_2 n \nabla r], \\ a_t &= \nabla \cdot [D_a \nabla a + \chi_2 a \nabla r] + k_1 n - k_2 a, \\ r_t &= D_r \nabla^2 r + k_3 n - k_4 r. \end{aligned} \quad (D10)$$

Balding and McElwain (1985) snail-trail model for angiogenic sprouting, for tip cells (n) and vessel cells (v) and chemoattractant (c):

$$\begin{aligned} n_t &= -\nabla \cdot [n \chi \nabla c] + k_1 c v - k_2 n v, \\ v_t &= |n \chi \nabla c| - k_3 v, \\ c_t &= D \nabla^2 c. \end{aligned} \quad (D11)$$

Note that it is assumed the chemical is produced at the tumour boundary at a constant rate, generating a source boundary condition for c .

Owen and Sherratt (1997) model for tumour-macrophage interactions, for macrophages (l), mutant cells (m), normal cells (n), chemical regulator (f) and macrophage-mutant complex (c):

$$\begin{aligned} l_t &= \nabla \cdot [D_l \nabla l - \chi l \nabla f] + \frac{k_1 f l (k_2 + k_3)}{k_4 + l + m + n} - k_5 (1 + k_6 f) - k_7 f l m + k_8 e - k_9 l, \\ m_t &= D_m \nabla^2 m + \frac{k_{10} f l (k_2 + k_3)}{k_4 + l + m + n} - k_{11} m - k_7 f l m, \\ n_t &= D_n \nabla^2 n + \frac{k_{11} f l (k_2 + k_3)}{k_4 + l + m + n} - k_{11} n, \\ f_t &= D_f \nabla^2 f + k_{12} m - k_{13} f, \\ c_t &= D_c \nabla^2 c + k_7 f l m - k_{14} c - k_{15} c. \end{aligned} \quad (D12)$$

Knútsdóttir et al. (2014) model for autocrine/paracrine macrophage-tumour interactions, for macrophages (m), tumour cells (n), CSF-1 concentration (c) and EGF concentration (e):

$$\begin{aligned} m_t &= \nabla \cdot [D_m \nabla m - \chi_1 m \nabla c], \\ n_t &= \nabla \cdot [D_n \nabla n - \chi_2 n \nabla e - \chi_3 n \nabla c], \\ c_t &= D_c \nabla^2 c + k_1 n - k_2 c, \\ e_t &= D_e \nabla^2 e + k_3 m - k_4 e. \end{aligned} \quad (\text{D13})$$

Chaplain and Lolas (2006) model for uPA mediated tumour invasion, for tumour cells (c), ECM (v) and uPA (u):

$$\begin{aligned} c_t &= \nabla \cdot [D_c \nabla c - \chi_1 c \nabla u - \chi_2 c \nabla v] + k_1 c(1 - k_2 c - k_3 v), \\ v_t &= -k_4 u v + k_5 v(1 - k_2 c - k_3 v), \\ u_t &= D_u \nabla^2 u + k_6 c - k_7 u. \end{aligned} \quad (\text{D14})$$

Appendix A.5. Models in ecology

Lee et al. (2009) model for predator-prey taxis, for predator (p) and prey (q):

$$\begin{aligned} p_t &= \nabla \cdot [D_p \nabla p - \chi(q) p \nabla q] + k_1 p(F(p, q) - G(p)), \\ q_t &= D_q \nabla^2 q + qH(q) - pF(p, q), \end{aligned} \quad (\text{E1})$$

where F, G, H are typical functions to describe predator-prey interactions.

Tania et al. (2012) model for forager-scrourger interactions, for forager (f), scrourger (s) and food resource (r):

$$\begin{aligned} f_t &= \nabla \cdot [D_f \nabla f - \chi_f f \nabla r] + G(f, s, r); \\ s_t &= \nabla \cdot [D_s \nabla s - \chi_s s \nabla f] + H(f, s, r); \\ r_t &= D_r \nabla^2 r + k_1 - k_2(f + s)r - k_3 r. \end{aligned} \quad (\text{E2})$$

Forager/scrourger kinetics G and H could be zero, follow standard population growth terms or be chosen to describe within species strategy switching.

Pearce et al. (2007) model for host-parasitoid chemotaxis systems, for two hosts (n, m), two parasites (p, q) and chemical (c):

$$\begin{aligned} n_t &= D_n \nabla^2 n + k_1 n(1 - n/k_2) - k_3 p(1 - e^{-k_4 n}), \\ m_t &= D_m \nabla^2 m + k_5 n(1 - n/k_6) - k_7 p(1 - e^{-k_8 m}) - k_9 q(1 - e^{-k_{10} m}), \\ p_t &= \nabla \cdot [D_p \nabla p - \chi_1 p \nabla c] + k_{11} p(1 - e^{-k_4 n}) + k_{12} p(1 - e^{-k_8 m}) - k_{13} p, \\ q_t &= \nabla \cdot [D_q \nabla q - \chi_2 q \nabla c] + k_{14} q(1 - e^{-k_{10} m}) - k_{15} q, \\ c_t &= D_c \nabla^2 c + k_{16}(n + m) - k_{17} c. \end{aligned} \quad (\text{E3})$$

Ramakrishnan et al. (2014) model for ant foraging behaviour, for foraging ants (u), ants returning from food source i (v_i) and pheromone (c):

$$\begin{aligned} u_t &= \nabla \cdot [\nabla u - u \nabla c] + k_1 F(x) \sum_{i=1}^n v_i - \sum_{i=1}^n \kappa_i G_i(x) u, \\ v_{it} &= -\nabla \cdot v_i \nabla F + \kappa_i G_i(x) u - k_1 F(x) v_i, \\ c_t &= D_c \nabla^2 c - c + \sum_{i=1}^n p_i u. \end{aligned} \quad (\text{E4})$$

Note that F is a vector denoting the nest direction.

Amorim (2015) model for ant foraging behaviour, for foraging ants (u), returning ants (w), pheromone (v) and food resource (c):

$$\begin{aligned} u_t &= \nabla \cdot [D_u \nabla u - \chi_u u \nabla v] - k_1 u c + k_2 w F(x) + G(t) F(x), \\ w_t &= \nabla \cdot [D_w \nabla w - \chi_w w \nabla A] + k_1 u c - k_2 w F(x), \\ v_t &= D_v \nabla^2 v + k_3 H(x) w - k_4 v; \\ c_t &= -k_5 u c. \end{aligned} \quad (\text{E5})$$

Note that $F(x)$ describes the location of the nest, $G(t)$ describes the rate of foraging ants emerging from the nest, $H(x)$ describes a decrease in pheromone deposition close to the nest and ∇A is an attraction to the nest. Logan et al. (1998) model for mountain pine beetle outbreaks, for flying beetles (b), nesting beetles (n), aggregation pheromone (a), host kairomones (c), tree resistance (r), and attack holes (h):

$$\begin{aligned}
b_t &= \nabla \cdot [D_b \nabla b - \chi_a b \nabla F(a) - \chi_c b \nabla c] + k_1 - k_2 b - k_3 \frac{r}{k_4} b (1 + k_5 a) , \\
n_t &= k_3 \frac{r}{k_4} b (1 + k_5 a) - k_6 n - k_7 n r , \\
a_t &= D_a \nabla^2 a + k_8 n - k_9 a , \\
c_t &= D_c \nabla^2 c + k_{10} h r - k_{11} c , \\
r_t &= r (k_{12} (k_{13} - r) - k_{14} h) , \\
h_t &= k_3 \frac{r}{k_4} b (1 + k_5 a) - k_{15} h r ,
\end{aligned} \tag{E6}$$

where $\nabla F(a) = \frac{k_{16} - a}{k_{16} + a / k_{17}} \nabla a$.

Strohm et al. (2013) model for mountain pine beetle outbreaks, for flying beetles (b), nesting beetles (n) and aggregation pheromone (a):

$$\begin{aligned}
b_t &= \nabla \cdot [D_b \nabla b - \chi b \frac{k_1 - a}{k_1 + a / k_2} \nabla a] + k_3 - k_4 b - k_5 b \frac{b^2}{b^2 + k_6^2} , \\
n_t &= k_5 b \frac{b^2}{b^2 + k_6^2} - k_7 n , \\
a_t &= D_a \nabla^2 a + k_8 n - k_9 a .
\end{aligned} \tag{E6}$$

Appendix A.6. Models in sociology

Neto and Claeysen (2015) model for capital-labour dynamics, for capital (c) and labour (l):

$$\begin{aligned}
l_t &= \nabla \cdot [D_l \nabla l - \chi l \nabla c] + k_1 l (1 - l / k_2) , \\
c_t &= D_c \nabla^2 c + k_3 c^q l^{1-q} - k_4 c .
\end{aligned} \tag{F1}$$

Short et al. (2008) model for crime hotspot formation, for criminals (c) and attractivity (a, b):

$$\begin{aligned}
c_t &= D_c \nabla \cdot [\nabla c - \frac{2c}{b+a} \nabla (b+a)] + k_1 - c(b+a) , \\
a_t &= D_a \nabla^2 a + k_2 c(b+a) - k_3 a .
\end{aligned} \tag{F2}$$

Note that the attractivity is decomposed into background level ($b(\mathbf{x})$) and the dynamic component (a).

Pitcher (2010) model for crime hotspot formation, for criminals (c), attractivity (a, b) and deterrent (d , policing):

$$\begin{aligned}
c_t &= D_c \nabla \cdot [\nabla c - \frac{2c}{a(1-d)^+} \nabla a(1-d)^+] + k_1 - k_2 c , \\
a_t &= D_a \nabla^2 (a-b) + k_3 c a (1-d)^+ (1-a/k_4) - k_5 (a-b) , \\
d_t &= D_d \nabla^2 d + k_6 u(\mathbf{x}, t) - k_7 d
\end{aligned} \tag{F3}$$

where $u(t, \mathbf{x})$ describes deterrence, subject to resource constraint $\int_{\Omega} u d\mathbf{x} = k_8$.

References

References

- J. Adler. Chemotaxis in bacteria. *Science*, 153:708–716, 1966.
J. Adler. Chemoreceptors in bacteria. *Science*, 166:1588–1597, 1969.
M. Aida, T. Tsujikawa, M. Efendiev, A. Yagi, and M. Mimura. Lower estimate of the attractor dimension for a chemotaxis growth system. *J. Lond. Math. Soc.*, 74:453–474, 2006.
M. Alber, N. Chen, P. M. Lushnikov, and S. A. Newman. Continuous macroscopic limit of a discrete stochastic model for interaction of living cells. *Phys. Rev. Lett.*, 99:168102, 2007.

- F. Alcantara and M. Monk. Signal propagation during aggregation in the slime mould *Dictyostelium discoideum*. *Microbiology*, 85: 321–334, 1974.
- W. Alt. Biased random walk models for chemotaxis and related diffusion approximations. *J. Math. Biol.*, 9:147–177, 1980.
- D. Ambrosi, F. Bussolino, and L. Preziosi. A review of vasculogenesis models. *J. Theor. Med.*, 6:1–19, 2005.
- P. Amorim. Modeling ant foraging: a chemotaxis approach with pheromones and trail formation. *J. Theor. Biol.*, 385:160–173, 2015.
- A. R. A. Anderson and M. A.J. Chaplain. Continuous and discrete mathematical models of tumor-induced angiogenesis. *Bull. Math. Biol.*, 60:857–899, 1998.
- A. Aotani, M. Mimura, and T. Mollé. A model aided understanding of spot pattern formation in chemotactic *E. coli* colonies. *Jap. J. Indust. Appl. Math.*, 27:5–22, 2010.
- Aristotle. *History of Animals. Translated by D. W. Thompson*. 1907.
- A. Arndt. Rhizopodenstudien III. *Wilh. Roux Arch. Entwickl. Org.*, 136:681–744, 1937.
- L. Backstrom, D. Huttenlocher, J. Kleinberg, and X. Lan. Group formation in large social networks: membership, growth, and evolution. In *Proc. 12th ACM SIGKDD international conference on Knowledge discovery and data mining*, pages 44–54, 2006.
- D. Balding and D. L. S. McElwain. A mathematical model of tumour-induced capillary growth. *J. Theor. Biol.*, 114:53–73, 1985.
- S. Banerjee, A. P. Misra, and L. Rondoni. Spatiotemporal evolution in a (2+1)-dimensional chemotaxis model. *Physica A*, 391: 107–112, 2012.
- R. Baronas, Ž. Ledas, and R. Šimkus. Computational modeling of the bacterial self-organization in a rounded container: the effect of dimensionality. *Nonlin. Anal. Model. Cont.*, 20, 2015.
- N. Bellomo, A. Bellouquid, Y. Tao, and M. Winkler. Toward a mathematical theory of Keller–Segel models of pattern formation in biological tissues. *Math. Mod. Meth. Appl. Sci.*, 25:1663–1763, 2015.
- E. Ben-Jacob, I. Cohen, and H. Levine. Cooperative self-organization of microorganisms. *Adv. Phys.*, 49:395–554, 2000.
- K. Bentley, M. Jones, and B. Cruys. Predicting the future: towards symbiotic computational and experimental angiogenesis research. *Exp. Cell Res.*, 319:1240–1246, 2013.
- H. C. Berg. Chemotaxis in bacteria. *Ann. Rev. Biophys. Bioeng.*, 4:119–136, 1975.
- J. T. Bonner. *The social amoebae: the biology of cellular slime molds*. Princeton University Press, 2009.
- J. T. Bonner and L. J. Savage. Evidence for the formation of cell aggregates by chemotaxis in the development of the slime mold *Dictyostelium discoideum*. *J. Exp. Zool. A*, 106:1–26, 1947.
- C. Bonnet. *Oeuvres d'histoire naturelle et de philosophie*. Neuchatel, 1779.
- A. Borst and M. Heisenberg. Osmotopotaxis in *Drosophila melanogaster*. *J. Compar. Physiol. A*, 147:479–484, 1982.
- S. Boyden. The chemotactic effect of mixtures of antibody and antigen on polymorphonuclear leucocytes. *J. Exp. Med.*, 115:453–466, 1962.
- D. Bray, M. D. Levin, and K. Lipkow. The chemotactic behavior of computer-based surrogate bacteria. *Curr. Biol.*, 17:12–19, 2007.
- M. P. Brenner, L. S. Levitov, and E. O. Budrene. Physical mechanisms for chemotactic pattern formation by bacteria. *Biophys. J.*, 74: 1677–1693, 1998.
- T. Bretschneider, H. G. Othmer, and C. J. Weijer. Progress and perspectives in signal transduction, actin dynamics, and movement at the cell and tissue level: lessons from *Dictyostelium*. *Interface Focus*, 6:20160047, 2016.
- E. O. Budrene and H. C. Berg. Complex patterns formed by motile cells of *Escherichia coli*. *Nature*, 349:630–633, 1991.
- E. O. Budrene and H. C. Berg. Dynamics of formation of symmetrical patterns by chemotactic bacteria. *Nature*, 376:49–53, 1995.
- H. M. Byrne and M. R. Owen. A new interpretation of the Keller–Segel model based on multiphase modelling. *J. Math. Biol.*, 49: 604–626, 2004.
- Y.-Y. Chang. Cyclic 3', 5'-adenosine monophosphate phosphodiesterase produced by the slime mold *Dictyostelium discoideum*. *Science*, 161:57–59, 1968.
- M. A. J. Chaplain and G. Lolas. Mathematical modelling of cancer invasion of tissue: dynamic heterogeneity. *Netw. Heterog. Med.*, 1:399–439, 2006.
- M. A. J. Chaplain and A. M. Stuart. A model mechanism for the chemotactic response of endothelial cells to tumour angiogenesis factor. *IMA J. Math. Med. & Biol.*, 10:149–168, 1993.
- P.-H. Chavanis. A stochastic Keller–Segel model of chemotaxis. *Comm. Nonlin. Sci.*, 15:60–70, 2010.
- X. Chen, J. Hao, X. Wang, Y. Wu, and Y. Zhang. Stability of spiky solution of Keller–Segel's minimal chemotaxis model. *J. Diff. Eqns.*, 257:3102–3134, 2014.
- A. Chertock, K. Fellner, A. Kurganov, A. Lorz, and P. A. Markowich. Sinking, merging and stationary plumes in a coupled chemotaxis–fluid model: a high-resolution numerical approach. *J. Fluid Mech.*, 694:155–190, 2012.
- M. H. Cohen and A. Robertson. Wave propagation in the early stages of aggregation of cellular slime molds. *J. Theor. Biol.*, 31: 101–118, 1971a.
- M. H. Cohen and A. Robertson. Chemotaxis and the early stages of aggregation in cellular slime molds. *J. Theor. Biol.*, 31:119–130, 1971b.
- O. A. Croze, G. P. Ferguson, M. E. Cates, and W. C. K. Poon. Migration of chemotactic bacteria in soft agar: role of gel concentration. *Biophys. J.*, 101:525–534, 2011.
- T. J. Czaczkes, C. Grüter, and F. L. W. Ratnieks. Trail pheromones: an integrative view of their role in social insect colony organization. *Ann. Rev. Entomol.*, 60:581–599, 2015.
- G. Daghfous, W. W. Green, B. S. Zielinski, and R. Dubuc. Chemosensory-induced motor behaviors in fish. *Curr. Opin. Neurobiol.*, 22:223–230, 2012.
- J. C. Dallon and H. G. Othmer. A discrete cell model with adaptive signalling for aggregation of *Dictyostelium discoideum*. *Phil.*

- Trans. Roy. Soc. Lond. B*, 352:391–417, 1997.
- Y. Deleuze, C-Y. Chiang, M. Thiriet, and Tony W. H. Sheu. Numerical study of plume patterns in a chemotaxis–diffusion–convection coupling system. *Comp. & Fluid.*, 126:58–70, 2016.
- Y. Dolak and C. Schmeiser. The Keller–Segel model with logistic sensitivity function and small diffusivity. *SIAM J. Appl. Math.*, 66: 286–308, 2005.
- A. d’Onofrio. Spatiotemporal effects of a possible chemorepulsion of tumor cells by immune system effectors. *J. Theor. Biol.*, 296: 41–48, 2012.
- D. Dormann and C. J. Weijer. Propagating chemoattractant waves coordinate periodic cell movement in Dictyostelium slugs. *Development*, 128:4535–4543, 2001.
- M. R. D’Orsogna and M. Perc. Statistical physics of crime: A review. *Phys. Life Rev.*, 12:1–21, 2015.
- B. J. Duistermars, D. M. Chow, and M. A. Frye. Flies require bilateral sensory input to track odor gradients in flight. *Curr. Biol.*, 19: 1301–1307, 2009.
- A. J. Durston. Dictyostelium discoideum aggregation fields as excitable media. *J. Theor. Biol.*, 42:483–504, 1973.
- A. J. Durston. Dictyostelium: The mathematician’s organism. *Current Gen.*, 14:355–360, 2013.
- L. Edelstein. The propagation of fungal colonies: a model for tissue growth. *J. Theor. Biol.*, 98:679–701, 1982.
- S-I. Ei, H. Izuhara, and M. Mimura. Spatio-temporal oscillations in the Keller–Segel system with logistic growth. *Physica D*, 277: 1–21, 2014.
- T. W. Engelmann. Neue methode zur untersuchung der sauerstoffausscheidung pflanzlicher und thierischer organism. *Pfl. Arch. Ges. Physiol. Mens. Tiere*, 25:285–292, 1881a.
- T. W. Engelmann. Zur biologie der schizomyceten. *Pfl. Arch. Ges. Physiol. Mens. Tiere*, 26:537–545, 1881b.
- T. W. Engelmann. Bacterium photometricum. ein beitrag zur vergleichenden physiologie des licht- und farbennsinnes. *Pfl. Arch. Ges. Physiol. Mens. Tiere*, 30:95–124, 1883.
- C. A. Erickson and K. R. Olivier. Negative chemotaxis does not control quail neural crest cell dispersion. *Dev. Biol.*, 96:542–551, 1983.
- G. Estrada-Rodríguez, H. Gimperlein, and K. J. Painter. Fractional Patlak-Keller-Segel equations for chemotactic superdiffusion. *arXiv preprint arXiv:1708.02751*, 2017.
- J-H. Fabre. Souvenirs entomologiques. *Paris*, 1879.
- J-H. Fabre. *Fabre’s book of insects*. Dodd, Mead, 1921.
- S. R. Farkas and H. H. Shorey. Chemical trail-following by flying insects: a mechanism for orientation to a distant odor source. *Science*, 178:67–68, 1972.
- E. A. Ferguson, J. Matthiopoulos, R. H. Insall, and D. Husmeier. Inference of the drivers of collective movement in two cell types: Dictyostelium and melanoma. *J. Roy. Soc. Interface*, 13:20160695, 2016.
- T. D. Fitzgerald and J. T. Costa. Collective behavior in social caterpillars. In *Information processing in social insects*, pages 379–400. Springer, 1999.
- J. A. Flegg, S. N. Menon, P. K. Maini, and S. D. L. McElwain. On the mathematical modeling of wound healing angiogenesis in skin as a reaction-transport process. *Front. Physiol.*, 6, 2015.
- G. S. Fraenkel and D. L. Gunn. *The orientation of animals: Kineses, taxes and compass reactions*. Reprinted 1961, Dover Press., 1940.
- Q. Gaudry, K. I. Nagel, and R. I. Wilson. Smelling on the fly: sensory cues and strategies for olfactory navigation in Drosophila. *Curr. Opin. Neurobiol.*, 22:216–222, 2012.
- G. Gerisch. Cell aggregation and differentiation in Dictyostelium. *Curr. Top. Dev. Biol.*, 3:157–197, 1968.
- R. Gillitzer and M. Goebeler. Chemokines in cutaneous wound healing. *J. Leuk. Biol.*, 69:513–521, 2001.
- J. D. Glover, K. L. Wells, F. Matthäus, K. J. Painter, W. Ho, J. Riddell, J. A. Johansson, M. J. Ford, C. A. B. Jahoda, V. Klika, R. Mort, and D. J. Headon. Hierarchical patterning modes orchestrate hair follicle morphogenesis. *PLoS Biology*, 15:e2002117, 2017.
- A. Gomez-Marin and M. Louis. Active sensation during orientation behavior in the Drosophila larva: more sense than luck. *Curr. Opin. Neurobiol.*, 22:208–215, 2012.
- J. B. A. Green and J. Sharpe. Positional information and reaction-diffusion: two big ideas in developmental biology combine. *Development*, 142:1203–1211, 2015.
- J. W. Griffith, C. L. Sokol, and A. D. Luster. Chemokines and chemokine receptors: positioning cells for host defense and immunity. *Ann. Rev. Immunol.*, 32:659–702, 2014.
- J. D. Gross, M. J. Peacey, and D. J. Trevan. Signal emission and signal propagation during early aggregation in Dictyostelium discoideum. *J. Cell Sci.*, 22:645–656, 1976.
- Y. Gu, Q. Wang, and G. Yi. Stationary patterns and their selection mechanism of urban crime models with heterogeneous near-repeat victimization effect. *Eur. J. Appl. Math.*, 28:141–178, 2017.
- W. Hangartner. Spezifität und inaktivierung des spurpheromons von lasius fuliginosus latr. und orientierung der arbeiterinnen im duftfeld. *Zeit. für Verg. Physiol.*, 57:103–136, 1967.
- W. Hangartner. Structure and variability of the individual odor trail in solenopsis geminata fabr.(hymenoptera, formicidae). *J. Compar. Physiol. A*, 62:111–120, 1969.
- T. A. M. Heck, M. M. Vaeyens, and H. Van Oosterwyck. Computational models of sprouting angiogenesis and cell migration: towards multiscale mechanochemical models of angiogenesis. *Math. Mod. Nat. Phen.*, 10:108–141, 2015.
- T. Hillen and K. J. Painter. A users guide to PDE models for chemotaxis. *J. Math. Biol.*, 58:183–217, 2009.
- T. Hillen and A. Potapov. The one-dimensional chemotaxis model: global existence and asymptotic profile. *Math. Meth. Mod. Appl.*

- Sci.*, 27:1783–1801, 2004.
- A. J. Hillesdon, T. J. Pedley, and J. O. Kessler. The development of concentration gradients in a suspension of chemotactic bacteria. *Bull. Math. Biol.*, 57:299–344, 1995.
- W. Ho and D. J. Headon. Interacting cellular and molecular waves drive gain and loss of high fidelity feather patterning. *Working Title*, TBD:TBD, In preparation.
- T. Höfer, P. K. Maini, J. A. Sherratt, M. A. J. Chaplain, P. Chauvet, D. Metevier, P. C. Montes, and J. D. Murray. A resolution of the chemotactic wave paradox. *Appl. Math. Lett.*, 7:1–5, 1994.
- T. Hofer, J. A. Sherratt, and P. K. Maini. Dictyostelium discoideum: cellular self-organization in an excitable biological medium. *Proc. Roy. Soc. Lond. B*, 259:249–257, 1995.
- T. Höfer, J. A. Sherratt, and P. K. Maini. Cellular pattern formation during Dictyostelium aggregation. *Physica D*, 85:425–444, 1995.
- D. Horstmann. From 1970 until present: The Keller-Segel model in chemotaxis and its consequences I. *Jahresberichte der DMV*, 105: 103–165, 2003.
- P. Hunter. The inflammation theory of disease. *EMBO reports*, 13:968–970, 2012.
- Y. Iino and K. Yoshida. Parallel use of two behavioral mechanisms for chemotaxis in *Caenorhabditis elegans*. *J. Neurosci.*, 29: 5370–5380, 2009.
- P. B. Johnsen and J. H. Teeter. Spatial gradient detection of chemical cues by catfish. *J. Comp. Physiol. A*, 140:95–99, 1980.
- S. T. Johnston, M. J. Simpson, and R. E. Baker. Modelling the movement of interacting cell populations: a moment dynamics approach. *J. Theor. Biol.*, 370:81–92, 2015.
- P. A. Jones, P. J. Brantingham, and L. R. Chayes. Statistical models of criminal behavior: the effects of law enforcement actions. *Math. Mod. Meth. Appl. Sci.*, 20:1397–1423, 2010.
- D. Kaiser. Coupling cell movement to multicellular development in myxobacteria. *Nat. Rev. Microbiol.*, 1:45–54, 2003.
- K. Kang, T. Kolokolnikov, and M. J. Ward. The stability and dynamics of a spike in the 1D Keller–Segel model. *IMA J. Appl. Math.*, 72:140–162, 2007.
- P. Kareiva and G. Odell. Swarms of predators exhibit “preytaxis” if individual predators use area-restricted search. *Am. Nat.*, 130: 233–270, 1987.
- E.F. Keller and L.A. Segel. Initiation of slime mold aggregation viewed as an instability. *J. Theor. Biol.*, 26:399–415, 1970.
- E.F. Keller and L.A. Segel. Model for chemotaxis. *J. Theor. Biol.*, 30:225–234, 1971a.
- E.F. Keller and L.A. Segel. Traveling bands of chemotactic bacteria: A theoretical analysis. *J. Theor. Biol.*, 30:377–380, 1971b.
- H. U. Keller, P. C. Wilkinson, M. Abercrombie, E. L. Becker, J. G. Hirsch, M. E. Miller, W. S. Ramsey, and S. H. Zigmond. A proposal for the definition of terms related to locomotion of leucocytes and other cells. *Cell Biol. Int. Rep.*, 1:391–397, 1977.
- R. H. Khonsari and V. Calvez. The origins of concentric demyelination: self-organization in the human brain. *PLoS One*, 2:e150, 2007.
- H. Knútsdóttir, E. Pálsson, and L. Edelstein-Keshet. Mathematical model of macrophage-facilitated breast cancer cells invasion. *J. Theor. Biol.*, 357:184–199, 2014.
- A. L. Kolodkin and M. Tessier-Lavigne. Mechanisms and molecules of neuronal wiring: a primer. *Cold Spring Harb. Persp. Biol.*, 3: a001727, 2011.
- T. M. Konijn, D. S. Barkley, Y. Y. Chang, and J. T. Bonner. Cyclic AMP: a naturally occurring acrasin in the cellular slime molds. *Am. Nat.*, 102:225–233, 1968.
- A. Kühn. *Die Orientierung der Tiere im Raum*. G. Fischer Jena, 1919.
- K. A. Landman, G. J. Pettet, and D. F. Newgreen. Mathematical models of cell colonization of uniformly growing domains. *Bull. Math. Biol.*, 65:235–262, 2003.
- I. R. Lapidus and R. Schiller. A model for traveling bands of chemotactic bacteria. *Biophys. J.*, 22:1–13, 1978.
- D. Lauffenburger and R. Aris. Measurement of leukocyte motility and chemotaxis parameters using a quantitative analysis of the under-agarose migration assay. *Math. Biosci.*, 44:121–138, 1979.
- D. Lauffenburger and K. H. Keller. Effects of leukocyte random motility and chemotaxis in tissue inflammatory response. *J. Theor. Biol.*, 81:475–503, 1979.
- D. Lauffenburger, C. R. Kennedy, and R. Aris. Traveling bands of chemotactic bacteria in the context of population growth. *Bull. Math. Biol.*, 46:19–40, 1984.
- D. A. Lauffenburger and C. R. Kennedy. Localized bacterial infection in a distributed model for tissue inflammation. *J. Math. Biol.*, 16:141–163, 1983.
- T. Leber. Über die entzndung und die wirkung der entzündungserregenden schädlichkeiten. *Fortschr. Med.*, 6:460–464, 1888.
- H. G. Lee and J. Kim. Numerical investigation of falling bacterial plumes caused by bioconvection in a three-dimensional chamber. *Eur. J. Mech. B*, 52:120–130, 2015.
- J. M. Lee, T. Hillen, and M. A. Lewis. Continuous traveling waves for prey-taxis. *Bull. Math. Biol.*, 70:654–676, 2008.
- J. M. Lee, T. Hillen, and M. A. Lewis. Pattern formation in prey-taxis systems. *J. Biol. Dyn.*, 3:551–573, 2009.
- S. Lee, S. Kim, Y. Oh, and H. J. Hwang. Mathematical modeling and its analysis for instability of the immune system induced by chemotaxis. *J. Math. Biol.*, 75:1101–1131, 2017.
- H. A. Levine, B. D. Sleeman, and M. Nilsen-Hamilton. Mathematical modeling of the onset of capillary formation initiating angiogenesis. *J. Math. Biol.*, 42:195–238, 2001.
- C-M. Lin, T. X. Jiang, R. E. Baker, P. K. Maini, R. B. Widelitz, and C-M. Chuong. Spots and stripes: pleomorphic patterning of stem cells via p-ERK-dependent cell chemotaxis shown by feather morphogenesis and mathematical simulation. *Dev. Biol.*, 334:

- 369–382, 2009.
- C-S. Lin, W-M. Ni, and I. Takagi. Large amplitude stationary solutions to a chemotaxis system. *J. Diff. Eqns.*, 72:1–27, 1988.
- S. R. Lockery. The computational worm: spatial orientation and its neuronal basis in *C. elegans*. *Curr. Opin. Neurobiol.*, 21:782–790, 2011.
- J. A. Logan, P. White, B. J. Bentz, and J. A. Powell. Model analysis of spatial patterns in mountain pine beetle outbreaks. *Theor. Pop. Biol.*, 53:236–255, 1998.
- M. C. Lombardo, R. Barresi, E. Bilotta, F. Gargano, P. Pantano, and M. Sammartino. Demyelination patterns in a mathematical model of multiple sclerosis. *J. Math. Biol.*, 75:373–417, 2017.
- M. Luca, A. Chavez-Ross, L. Edelstein-Keshet, and Alex Mogilner. Chemotactic signaling, microglia, and alzheimers disease senile plaques: Is there a connection? *Bull. Math. Biol.*, 65:693–730, 2003.
- M. Machado, M. G. Watson, A. H. Devlin, M. A. J. Chaplain, S. R. McDougall, and C. A. Mitchell. Dynamics of angiogenesis during wound healing: a coupled in vivo and in silico study. *Microcirculation*, 18:183–197, 2011.
- P. K. Maini, M. R. Myerscough, K. H. Winters, and J. D. Murray. Bifurcating spatially heterogeneous solutions in a chemotaxis model for biological pattern generation. *Bull. Math. Biol.*, 53:701–719, 1991.
- N. V. Mantzaris, S. Webb, and H. G. Othmer. Mathematical modeling of tumor-induced angiogenesis. *J. Math. Biol.*, 49:111–187, 2004.
- A. F. M. Marée and P. Hogeweg. How amoeboids self-organize into a fruiting body: multicellular coordination in *Dictyostelium discoideum*. *Proc. Natl. Acad. Sci.*, 98:3879–3883, 2001.
- H. Martin. Osmotropotaxis in the honey-bee. *Nature*, 208:59–63, 1965.
- R. F. Mathewson and E. S. Hodgson. Klinotaxis and rheotaxis in orientation of sharks toward chemical stimuli. *Comp. Biochem. Physiol. A*, 42:79–82, 1972.
- S. Matsukuma and A. J. Durston. Chemotactic cell sorting in *Dictyostelium discoideum*. *Development*, 50:243–251, 1979.
- S. R. McDougall, M. G. Watson, A. H. Devlin, C. A. Mitchell, and M. A. J. Chaplain. A hybrid discrete-continuum mathematical model of pattern prediction in the developing retinal vasculature. *Bull. Math. Biol.*, 74:2272–2314, 2012.
- R. McLennan, J. M. Teddy, J. C. Kasemeier-Kulesa, M. H. Romine, and P. M. Kulesa. Vascular endothelial growth factor (VEGF) regulates cranial neural crest migration in vivo. *Dev. Biol.*, 339:114–125, 2010.
- E. Metchnikoff. *Leçons sur la pathologie comparée de l’inflammation: faites à l’Institut Pasteur en avril et mai 1891*. G. Masson, 1892.
- F. Michon, L. Forest, E. Collomb, J. Demongeot, and D. Dhouailly. BMP2 and BMP7 play antagonistic roles in feather induction. *Development*, 135:2797–2805, 2008.
- M. Mimura and T. Tsujikawa. Aggregating pattern dynamics in a chemotaxis model including growth. *Physica A*, 230:499–543, 1996.
- Y. Mishima and M. Lotz. Chemotaxis of human articular chondrocytes and mesenchymal stem cells. *J. Orthopaed. Res.*, 26:1407–1412, 2008.
- N. Mittal, E. O. Budrene, M. P. Brenner, and A. Van Oudenaarden. Motility of *Escherichia coli* cells in clusters formed by chemotactic aggregation. *Proc. Nat. Acad. Sci. USA*, 100:13259–13263, 2003.
- P. B. Monk and H. G. Othmer. Wave propagation in aggregation fields of the cellular slime mould *Dictyostelium discoideum*. *Proc. Roy. Soc. Lond. B*, 240:555–589, 1990.
- D. J. Montell, W. H. Yoon, and M. Starz-Gaiano. Group choreography: mechanisms orchestrating the collective movement of border cells. *Nat. Rev. Mol. Cell Biol.*, 13:631, 2012.
- D. F. Morey. The early evolution of the domestic dog. *Am. Sci.*, pages 336–347, 1994.
- J. D. Murray. *Mathematical Biology. II Spatial Models and Biomedical Applications*. Springer-Verlag, New York, 2003.
- J. D. Murray and M. R. Myerscough. Pigmentation pattern formation on snakes. *J. Theor. Biol.*, 149:339–360, 1991.
- M. R. Myerscough, P. K. Maini, and K. J. Painter. Pattern formation in a generalized chemotactic model. *Bull. Math. Biol.*, 60:1–26, 1998.
- V. Nanjundiah. Chemotaxis, signal relaying and aggregation morphology. *J. Theor. Biol.*, 42:63–105, 1973.
- J. P. J. Neto and J. C. R. Claeyssen. Capital-induced labor migration in a spatial Solow model. *J. Econom.*, 115:25–47, 2015.
- T. J. Newman and R. Grima. Many-body theory of chemotactic cell-cell interactions. *Phys. Rev. E*, 70:051916, 2004.
- J. M. E. Nichols, D. Veltman, and R. R. Kay. Chemotaxis of a model organism: progress with *Dictyostelium*. *Curr. Opin. Cell Biol.*, 36:7–12, 2015.
- G. M. Odell and J. T. Bonner. How the *Dictyostelium discoideum* grex crawls. *Phil. Trans. Roy. Soc. Lond. B*, 312:487–525, 1986.
- M. E. Orme and M. A. J. Chaplain. A mathematical model of the first steps of tumour-related angiogenesis: capillary sprout formation and secondary branching. *IMA Math. Med. & Biol.*, 13:73–98, 1996.
- G. F. Oster and J. D. Murray. Pattern formation models and developmental constraints. *J. Exp. Zool. A*, 251:186–202, 1989.
- H. G. Othmer and T. Hillen. The diffusion limit of transport equations II: Chemotaxis equations. *SIAM J. Appl. Math.*, 62:1222–1250, 2002.
- H. G. Othmer and P. Schaap. Oscillatory cAMP signaling in the development of *Dictyostelium discoideum*. *Comm. Theor. Biol.*, 5: 175–282, 1998.
- H. G. Othmer and C. Xue. The mathematical analysis of biological aggregation and dispersal: progress, problems and perspectives. In *Dispersal, Individual Movement and Spatial Ecology*, pages 79–127. Springer, 2013.
- H. G. Othmer, S. R. Dunbar, and W. Alt. Models of dispersal in biological systems. *J. Math. Biol.*, 26:263–298, 1988.
- H. G. Othmer, X. Xin, and C. Xue. Excitation and adaptation in bacteria—a model signal transduction system that controls taxis and spatial pattern formation. *Int. J. Mol. Sci.*, 14:9205–9248, 2013.

- M. R. Owen and J. A. Sherratt. Pattern formation and spatiotemporal irregularity in a model for macrophage–tumour interactions. *J. Theor. Biol.*, 189:63–80, 1997.
- K. J. Painter. Continuous models for cell migration in tissues and applications to cell sorting via differential chemotaxis. *Bull. Math. Biol.*, 71:1117–1147, 2009.
- K. J. Painter and T. Hillen. Spatio-temporal chaos in a chemotaxis model. *Physica D*, 240:363–375, 2011.
- K. J. Painter and J. A. Sherratt. Modelling the movement of interacting cell populations. *J. Theor. Biol.*, 225:327–339, 2003.
- K. J. Painter, P. K. Maini, and H. G. Othmer. Stripe formation in juvenile *Pomacanthus* explained by a generalized Turing mechanism with chemotaxis. *Proc. Natl. Acad. Sci. USA*, 96:5549–5554, 1999.
- K. J. Painter, P. K. Maini, and H. G. Othmer. A chemotactic model for the advance and retreat of the primitive streak in avian development. *Bull. Math. Biol.*, 62:501–525, 2000.
- K. J. Painter, G. S. Hunt, K. L. Wells, J. A. Johansson, and D. J. Headon. Towards an integrated experimental–theoretical approach for assessing the mechanistic basis of hair and feather morphogenesis. *Interface Focus*, 2:433–450, 2012.
- K. J. Painter, W. Ho, and D. J. Headon. A chemotaxis model of feather primordia pattern formation during avian development. *J. Theor. Biol.*, 437:225–238, 2018.
- E. Palsson and H. G. Othmer. A model for individual and collective cell movement in *Dictyostelium discoideum*. *Proc. Natl. Acad. Sci. USA*, 97:10448–10453, 2000.
- P. Pan, E. M. Hall, and J. T. Bonner. Determination of the active portion of the folic acid molecule in cellular slime mold chemotaxis. *J. Bacteriol.*, 122:185–191, 1975.
- J. S. Parkinson, G. L. Hazelbauer, and J. J. Falke. Signaling and sensory adaptation in *Escherichia coli* chemoreceptors: 2015 update. *Trends Microbiol.*, 23:257–266, 2015.
- E. F. Pate and H. G. Othmer. Differentiation, cell sorting and proportion regulation in the slug stage of *Dictyostelium discoideum*. *J. Theor. Biol.*, 118:301–319, 1986.
- C. S. Patlak. Random walk with persistence and external bias. *Bull. Math. Biophys.*, 15:311–338, 1953a.
- C. S. Patlak. A mathematical contribution to the study of orientation of organisms. *Bull. Math. Biophys.*, 15:431–476, 1953b.
- I. G. Pearce, M. A. J. Chaplain, P. G. Schofield, A. R. A. Anderson, and S. F. Hubbard. Chemotaxis-induced spatio-temporal heterogeneity in multi-species host-parasitoid systems. *J. Math. Biol.*, 55:365–388, 2007.
- K. Pearson. The problem of the random walk. *Nature*, 72:294, 1905.
- K. Pearson. A mathematical theory of random migration, mathematical contributions to the theory of evolution XV. *Drapers Company Research Memoirs, Biometric Series. Dulau and Co, London*, 1906.
- K. Penner, B. Ermentrout, and D. Swigon. Pattern formation in a model of acute inflammation. *SIAM J. Appl. Dyn. Sys.*, 11:629–660, 2012.
- A. Perna, B. Granovskiy, S. Garnier, S. C. Nicolis, M. Labédan, G. Theraulaz, V. Fourcassié, and D. J. T. Sumpter. Individual rules for trail pattern formation in Argentine ants (*Linepithema humile*). *PLoS Comp. Biol.*, 8:e1002592, 2012.
- B. Perthame. *Transport equations in biology*. Springer Science & Business Media, 2006.
- B. Perthame, N. Vauchelet, and Z. Wang. The flux limited keller-segel system; properties and derivation from kinetic equations. *arXiv preprint arXiv:1801.07062*, 2018.
- W. F. Pfeffer. Locomotorische richtungsbewegungen durch chemische reize. *Unters. Bot. Inst. Tübingen*, 1:363–482, 1884.
- J. T. Pierce-Shimomura, T. M. Morse, and S. R. Lockery. The fundamental role of pirouettes in *Caenorhabditis elegans* chemotaxis. *J. Neurosci.*, 19:9557–9569, 1999.
- S. Pillay, H. M. Byrne, and P. K. Maini. Modeling angiogenesis: A discrete to continuum description. *Phys. Rev. E*, 95:012410, 2017.
- M. Pineda, C. J. Weijer, and R. Eftimie. Modelling cell movement, cell differentiation, cell sorting and proportion regulation in *Dictyostelium discoideum* aggregations. *J. Theor. Biol.*, 370:135–150, 2015.
- A. B. Pitcher. Adding police to a mathematical model of burglary. *Eur. J. Appl. Math.*, 21:401–419, 2010.
- A. A. Polezhaev, R. A. Pashkov, A. I. Lobanov, and I. B. Petrov. Spatial patterns formed by chemotactic bacteria *Escherichia coli*. *Int. J. Dev. Biol.*, 50:309–314, 2006.
- J. Porter, B. Craven, R. M. Khan, S.-J. Chang, I. Kang, B. Judkewitz, J. Volpe, G. Settles, and N. Sobel. Mechanisms of scent-tracking in humans. *Nat. Neurosci.*, 10:27–29, 2007.
- A. B. Potapov and T. Hillen. Metastability in chemotaxis models. *J. Dyn. Diff. Eq.*, 17:293–330, 2005.
- J. Powell, J. Tams, B. Bentz, and J. Logan. Theoretical analysis of “switching” in a localized model for mountain pine beetle mass attack. *J. Theor. Biol.*, 194:49–63, 1998.
- J. A. Powell, J. A. Logan, and B. J. Bentz. Local projections for a global model of mountain pine beetle attacks. *J. Theor. Biol.*, 179:243–260, 1996.
- R. Rajan, J. P. Clement, and U. S. Bhalla. Rats smell in stereo. *Science*, 311:666–670, 2006.
- S. Ramakrishnan, T. Laurent, M. Kumar, and A. L. Bertozzi. Spatiotemporal chemotactic model for ant foraging. *Mod. Phys. Lett. B*, 28:1450238, 2014.
- S. Ramon y Cajal. La rétine des vertébrés. *La Cellule*, 9:121–133, 1892.
- K. B. Raper. *Dictyostelium discoideum*, a new species of slime mold from decaying forest leaves. *J. Agricul. Res.*, 50:135–147, 1935.
- S. Rasmann, J. G. Ali, J. Helder, and W. H. van der Putten. Ecology and evolution of soil nematode chemotaxis. *J. Chem. Ecol.*, 38:615–628, 2012.
- P. B. Reeder and B. W. Ache. Chemotaxis in the florida spiny lobster, *Panulirus argus*. *Anim. Behav.*, 28:831–839, 1980.
- J. Rennie. *Insect Miscellanies*. 1831.
- M. A. Rivero, R. T. Tranquillo, H. M. Buettner, and D. A. Lauffenburger. Transport models for chemotactic cell populations based on

- individual cell behavior. *Chem. Eng. Sci.*, 44:2881–2897, 1989.
- E. T. Roussos, J. S. Condeelis, and A. Patsialou. Chemotaxis in cancer. *Nat. Rev. Cancer*, 11:573–587, 2011.
- E. H. Runyon. Aggregation of separate cells of Dictyostelium to form a multicellular body. *Collecting Net*, 17:88, 1942.
- J. Saragosti, V. Calvez, N. Bournaveas, B. Perthame, A. Buguin, and P. Silberzan. Directional persistence of chemotactic bacteria in a traveling concentration wave. *Proc. Natl. Acad. Sci. USA*, 108:16235–16240, 2011.
- N. J. Savill and P. Hogeweg. Modelling morphogenesis: from single cells to crawling slugs. *J. Theor. Biol.*, 184:229–235, 1997.
- M. J. Schnitzer, S. M. Block, and H. C. Berg. Strategies for chemotaxis. *Biology of the Chemotactic Response*, 46:15–34, 1990.
- K. Schwenk. Why snakes have forked tongues. *Science*, 263:1573–1577, 1994.
- M. Scianna, C. G. Bell, and L. Preziosi. A review of mathematical models for the formation of vascular networks. *J. Theor. Biol.*, 333:174–209, 2013.
- L. A. Segel, A. S. Perelson, J. M. Hyman, and S. N. Klaus. Rash theory. In *Theoretical and Experimental Insights into Immunology*, pages 333–352. Springer, 1992.
- H. H. P. Severin and H. C. Severin. Behavior of the Mediterranean fruit fly (*Ceratitis capitata* Wied.) towards kerosene. *J. Anim. Behav.*, 4:223–227, 1914.
- B. M. Shaffer. Aggregation in cellular slime moulds: in vitro isolation of acrasin. *Nature*, 171:975–975, 1953.
- B. M. Shaffer. Acrasin, the chemotactic agent in cellular slime moulds. *J. Exp. Biol.*, 33:645–657, 1956.
- B. M. Shaffer. Aspects of aggregation in cellular slime moulds 1. Orientation and chemotaxis. *Am. Nat.*, 91:19–35, 1957.
- B. M. Shaffer. The cells founding aggregation centres in the slime mould *Polysphondylium violaceum*. *J. Exp. Biol.*, 38:833–849, 1961.
- B. M. Shaffer. Secretion of cyclic AMP induced by cyclic AMP in the cellular slime mould *Dictyostelium discoideum*. *Nature*, 255:549–552, 1975.
- J. A. Shapiro. Thinking about bacterial populations as multicellular organisms. *Ann. Rev. Microbiol.*, 52:81–104, 1998.
- A. Shellard and R. Mayor. Chemotaxis during neural crest migration. *Sem. Cell & Dev. Biol.*, 55:111–118, 2016.
- J. A. Sherratt. Chemotaxis and chemokinesis in eukaryotic cells: the Keller-Segel equations as an approximation to a detailed model. *Bull. Math. Biol.*, 56:129–146, 1994.
- M. B. Short, M. R. D’Orsogna, V. B. Pasour, G. E. Tita, P. J. Brantingham, A. L. Bertozzi, and L. B. Chayes. A statistical model of criminal behavior. *Math. Mod. Meth. Appl. Sci.*, 18:1249–1267, 2008.
- M. B. Short, A. L. Bertozzi, and P. J. Brantingham. Nonlinear patterns in urban crime: Hotspots, bifurcations, and suppression. *SIAM J. Appl. Dyn. Sys.*, 9:462–483, 2010a.
- M. B. Short, P. J. Brantingham, A. L. Bertozzi, and G. E. Tita. Dissipation and displacement of hotspots in reaction-diffusion models of crime. *Proc. Nat. Acad. Sci. USA*, 107:3961–3965, 2010b.
- A. N. Silchenko and P. A. Tass. Mathematical modeling of chemotaxis and glial scarring around implanted electrodes. *New J. Phys.*, 17:023009, 2015.
- M. J. Simpson, K. A. Landman, B. D. Hughes, and D. F. Newgreen. Looking inside an invasion wave of cells using continuum models: proliferation is the key. *J. Theor. Biol.*, 243:343–360, 2006.
- M. J. Simpson, K. A. Landman, and B. D. Hughes. Multi-species simple exclusion processes. *Physica A*, 388:399–406, 2009.
- H-K. Song, S-H. Lee, and P. F. Goetinck. FGF-2 signaling is sufficient to induce dermal condensations during feather development. *Dev. Dyn.*, 231:741–749, 2004.
- O. Stancevic, C. N. Angstmann, J. M. Murray, and B. I. Henry. Turing patterns from dynamics of early HIV infection. *Bull. Math. Biol.*, 75:774–795, 2013.
- J. Sternfeld and C. N. David. Cell sorting during pattern formation in Dictyostelium. *Differentiation*, 20:10–21, 1981.
- A. Stevens. The derivation of chemotaxis equations as limit dynamics of moderately interacting stochastic many-particle systems. *SIAM J. Appl. Math.*, 61:183–212, 2000.
- A. Stevens and H. G. Othmer. Aggregation, blowup, and collapse: the ABC’s of taxis in reinforced random walks. *SIAM J. Appl. Math.*, 57:1044–1081, 1997.
- C. L. Stokes and D. A. Lauffenburger. Analysis of the roles of microvessel endothelial cell random motility and chemotaxis in angiogenesis. *J. Theor. Biol.*, 152:377–403, 1991.
- J. E. Strassmann, Y. Zhu, and D. C. Queller. Altruism and social cheating in the social amoeba *Dictyostelium discoideum*. *Nature*, 408:965–967, 2000.
- S. Strohm, R. C. Tyson, and J. A. Powell. Pattern formation in a model for mountain pine beetle dispersal: Linking model predictions to data. *Bull. Math. Biol.*, 75:1778–1797, 2013.
- N. Tania, B. Vanderlei, J. P. Heath, and L. Edelstein-Keshet. Role of social interactions in dynamic patterns of resource patches and forager aggregation. *Proc. Natl. Acad. Sci. USA*, 109:11228–11233, 2012.
- M. Tessier-Lavigne and C. S. Goodman. The molecular biology of axon guidance. *Science*, 274:1123–1133, 1996.
- R. Thar and M. Köhl. Bacteria are not too small for spatial sensing of chemical gradients: an experimental evidence. *Proc. Natl. Acad. Sci. USA*, 100:5748–5753, 2003.
- E. Theveneau, L. Marchant, S. Kuriyama, M. Gull, B. Moepps, M. Parsons, and R. Mayor. Collective chemotaxis requires contact-dependent cell polarity. *Dev. Cell*, 19:39–53, 2010.
- M. J. Tindall, P. K. Maini, S. L. Porter, and J. P. Armitage. Overview of mathematical approaches used to model bacterial chemotaxis II: bacterial populations. *Bull. Math. Biol.*, 70:1570–1607, 2008a.
- M. J. Tindall, S. L. Porter, P. K. Maini, G. Gaglia, and J. P. Armitage. Overview of mathematical approaches used to model bacterial chemotaxis I: the single cell. *Bull. Math. Biol.*, 70:1525–1569, 2008b.

- D. Traynor, R. H. Kessin, and J. G. Williams. Chemotactic sorting to cAMP in the multicellular stages of Dictyostelium development. *Proc. Nat. Acad. Sci. USA*, 89:8303–8307, 1992.
- G. R. Trevanius. *Biologie oder Philosophie der lebenden Natur für Naturforscher und Ante*, volume VI. Rower, Gottingen, 1822.
- L. Tsimring, H. Levine, I. Aranson, E. Ben-Jacob, I. Cohen, O. Shochet, and W. N. Reynolds. Aggregation patterns in stressed bacteria. *Phys. Rev. Lett.*, 75:1859, 1995.
- Y. Tu. Quantitative modeling of bacterial chemotaxis: signal amplification and accurate adaptation. *Ann. Rev. Biophys.*, 42:337–359, 2013.
- P. Turchin. Translating foraging movements in heterogeneous environments into the spatial distribution of foragers. *Ecology*, 72:1253–1266, 1991.
- A. M. Turing. The chemical basis of morphogenesis. *Phil. Trans. Roy. Soc. Lond. B*, 237:37–72, 1952.
- I. Tuval, L. Cisneros, C. Dombrowski, C. W. Wolgemuth, J. O. Kessler, and R. E. Goldstein. Bacterial swimming and oxygen transport near contact lines. *Proc. Natl. Acad. Sci. USA*, 102:2277–2282, 2005.
- V. C. Twitty. Chromatophore migration as a response to mutual influences of the developing pigment cells. *J. Exp. Zool. Part A*, 95:259–290, 1944.
- V. C. Twitty and M. C. Niu. Causal analysis of chromatophore migration. *J. Exp. Zool. A*, 108:405–437, 1948.
- V. C. Twitty and M. C. Niu. The motivation of cell migration, studied by isolation of embryonic pigment cells singly and in small groups in vitro. *J. Exp. Zool. A*, 125:541–573, 1954.
- J. J. Tyson, K. A. Alexander, V. S. Manoranjan, and J. D. Murray. Spiral waves of cyclic AMP in a model of slime mold aggregation. *Physica D*, 34:193–207, 1989.
- R. Tyson, S. R. Lubkin, and J. D. Murray. A minimal mechanism for bacterial pattern formation. *Proc. Roy. Soc. Lond B*, 266:299–304, 1999a.
- R. Tyson, S. R. Lubkin, and J. D. Murray. Model and analysis of chemotactic bacterial patterns in a liquid medium. *J. Math. Biol.*, 38:359–375, 1999b.
- P. J. M. Van Haastert and P. N. Devreotes. Chemotaxis: signalling the way forward. *Nat. Rev. Mol. Cell Biol.*, 5:626–634, 2004.
- C. Van Oss, A. V. Panfilov, P. Hogeweg, F. Siegert, and C. J. Weijer. Spatial pattern formation during aggregation of the slime mould Dictyostelium discoideum. *J. Theor. Biol.*, 181:203–213, 1996.
- B. Vasiev and C. J. Weijer. Modelling of Dictyostelium discoideum slug migration. *J. Theor. Biol.*, 223:347–359, 2003.
- D. K. Vig and C. W. Wolgemuth. Spatiotemporal evolution of erythema migrans, the hallmark rash of Lyme disease. *Biophys. J.*, 106:763–768, 2014.
- G. Von Békésy. Olfactory analogue to directional hearing. *J. Appl. Physiol.*, 19:369–373, 1964.
- C. H. Waddington. *The principles of embryology*. Macmillan, New York, 1956.
- G. H. Wadhams and J. P. Armitage. Making sense of it all: bacterial chemotaxis. *Nat. Rev. Mol. Cell Biol.*, 5:1024, 2004.
- Z. Wang. Mathematics of travelling waves in chemotaxis. *Disc. Cont. Dyn. Sys. B.*, 18:601–641, 2013.
- Z. Wang and T. Hillen. Classical solutions and pattern formation for a volume filling chemotaxis model. *Chaos*, 17:037108, 2007.
- S. Ward. Chemotaxis by the nematode Caenorhabditis elegans: identification of attractants and analysis of the response by use of mutants. *Proc. Natl. Acad. Sci. USA*, 70:817–821, 1973.
- E. O. Wilson. Chemical communication among workers of the fire ant Solenopsis saevissima (fr. smith) 1. the organization of mass-foraging. *Anim. Behav.*, 10:134–147, 1962.
- L. Wolpert. Positional information and the spatial pattern of cellular differentiation. *J. Theor. Biol.*, 25:1–47, 1969.
- D. E. Woodward, R. Tyson, M. R. Myerscough, J. D. Murray, E. O. Budrene, and H. C. Berg. Spatio-temporal patterns generated by Salmonella typhimurium. *Biophys. J.*, 68:2181–2189, 1995.
- C. Xue and H. G. Othmer. Multiscale models of taxis-driven patterning in bacterial populations. *SIAM J. Appl. Math.*, 70:133–167, 2009.
- C. Xue, E. O. Budrene, and H. G. Othmer. Radial and spiral stream formation in Proteus mirabilis colonies. *PLoS Comp. Biol.*, 7:e1002332, 2011.
- X. Yang, D. Dormann, A. E. Münsterberg, and C. J. Weijer. Cell movement patterns during gastrulation in the chick are controlled by positive and negative chemotaxis mediated by FGF4 and FGF8. *Dev. Cell*, 3:425–437, 2002.
- Y. Zhang, X. Chen, J. Hao, X. Lai, and C. Qin. Dynamics of spike in a Keller-Segel’s minimal chemotaxis model. *Disc. Cont. Dyn. Sys. B*, 37:1109–1127, 2017.
- J. R. Zipkin, M. B. Short, and A. L. Bertozzi. Cops on the dots in a mathematical model of urban crime and police response. *Disc. Cont. Dyn. Syst. B*, 19:1479–1506, 2014.